Elevated temperature iron-based hard-facing deformation

A correlative microscopy study

Ben Poole (IC), Daniele Dini (IC), David Stewart (RR), Fionn Dunne (IC)

Friction **5**(3): 263–284 (2017) ISSN 2223-7690
https://doi.org/10.1007/s40544-017-0183-5 CN 10-1237/TH

REVIEW ARTICLE

Influence of tribology on global energy consumption, costs and emissions

Kenneth HOLMBERG[1,*], **Ali ERDEMIR**[2]

[1] *VTT Technical Research Centre of Finland, VTT FI-02044, Finland*

[2] *Argonne National Laboratory, Argonne, IL 60439, USA*

Received: 17 May 2017 / Accepted: 06 July 2017

Abstract: Calculations of the impact of friction and wear on energy consumption, economic expenditure, and CO_2 emissions are presented on a global scale. This impact study covers the four main energy consuming sectors: transportation, manufacturing, power generation, and residential. Previously published four case studies on passenger cars, trucks and buses, paper machines and the mining industry were included in our detailed calculations as reference data in our current analyses. The following can be concluded:

– In total, ~23% (119 EJ) of the world's total energy consumption originates from tribological contacts. Of that 20% (103 EJ) is used to overcome friction and 3% (16 EJ) is used to remanufacture worn parts and spare equipment due to wear and wear-related failures.

– By taking advantage of the new surface, materials, and lubrication technologies for friction reduction and wear protection in vehicles, machinery and other equipment worldwide, energy losses due to friction and wear could potentially be reduced by 40% in the long term (15 years)and by 18% in the short term (8 years). On global scale, these savings would amount to 1.4% of the GDP annually and 8.7% of the total energy consumption in the long term.

– The largest short term energy savings are envisioned in transportation (25%) and in the power generation (20%) while the potential savings in the manufacturing and residential sectors are estimated to be ~10%. In the longer terms, the savings would be 55%, 40%, 25%, and 20%, respectively.

– Implementing advanced tribological technologies can also reduce the CO_2 emissions globally by as much as 1,460 $MtCO_2$ and result in 450,000 million Euros cost savings in the short term. In the longer term, the reduction can be 3,140 $MtCO_2$ and the cost savings 970,000 million Euros.

Fifty years ago, wear and wear-related failures were a major concern for UK industry and their mitigation was considered to be the major contributor to potential economic savings by as much as 95% in ten years by the development and deployment of new tribological solutions. The corresponding estimated savings are today still of the same orders but the calculated contribution to cost reduction is about 74% by friction reduction and to 26% from better wear protection. Overall, wear appears to be more critical than friction as it may result in

Friction **5**(3): 263–284 (2017) ISSN 2223-7690
https://doi.org/10.1007/s40544-017-0183-5 CN 10-1237/TH
REVIEW ARTICLE

Influence of tribology on global energy consumption, costs and emissions

Kenneth HOLMBERG[1,*], Ali ERDEMIR[2]
[1] *VTT Technical Research Centre of Finland, VTT FI-02044, Finland*
[2] *Argonne National Laboratory, Argonne, IL 60439, USA*
Received: 17 May 2017 / Accepted: 06 July 2017

Abstract: Calculations of the impact of friction and wear on energy consumption, economic expenditure, and CO_2 emissions are presented on a global scale. This impact study covers the four main energy consuming sectors:

– In total, ~23% (119 EJ) of the world’s total energy consumption originates from tribological contacts. Of that 20% (103 EJ) is used to overcome friction and 3% (16 EJ) is used to remanufacture worn parts and spare equipment due to wear and wear-related failures.

– By taking advantage of the new surface, materials, and lubrication technologies for friction reduction and wear protection in vehicles, machinery and other equipment worldwide, energy losses due to friction and wear could potentially be reduced by 40% in the long term (15 years)and by 18% in the short term (8 years). On global scale, these savings would amount to 1.4% of the GDP annually and 8.7% of the total energy consumption in the long term.

– The largest short term energy savings are envisioned in transportation (25%) and in the power generation (20%) while the potential savings in the manufacturing and residential sectors are estimated to be ~10%. In the longer terms, the savings would be 55%, 40%, 25%, and 20%, respectively.

– Implementing advanced tribological technologies can also reduce the CO_2 emissions globally by as much as 1,460 $MtCO_2$ and result in 450,000 million Euros cost savings in the short term. In the longer term, the reduction can be 3,140 $MtCO_2$ and the cost savings 970,000 million Euros.

Fifty years ago, wear and wear-related failures were a major concern for UK industry and their mitigation was considered to be the major contributor to potential economic savings by as much as 95% in ten years by the development and deployment of new tribological solutions. The corresponding estimated savings are today still of the same orders but the calculated contribution to cost reduction is about 74% by friction reduction and to 26% from better wear protection. Overall, wear appears to be more critical than friction as it may result in

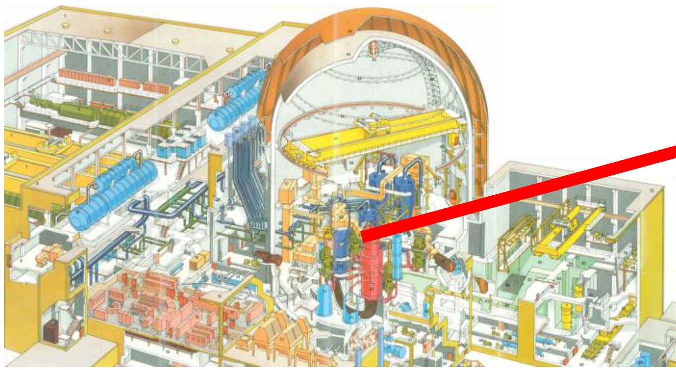

Pressurised water reactor

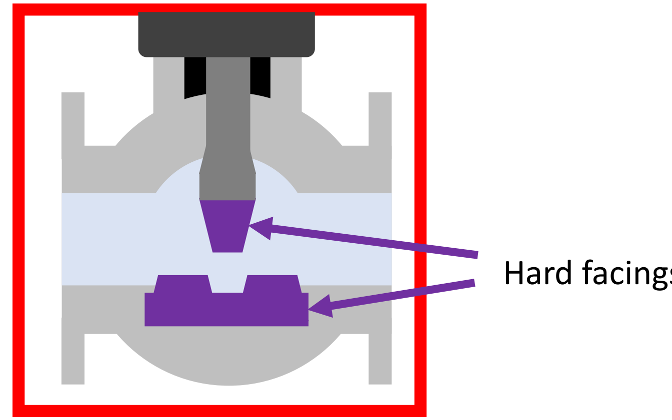

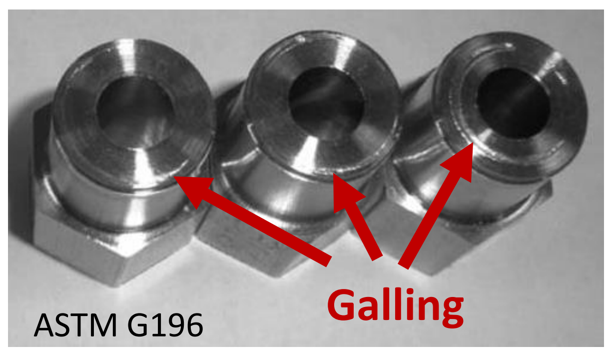

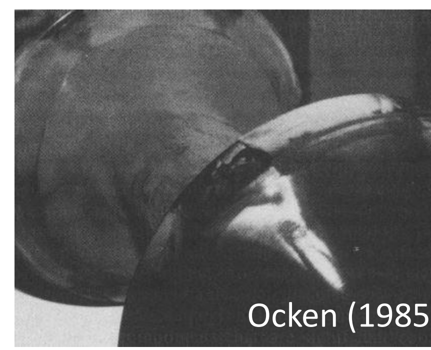

Ocken, Howard. "Reducing the cobalt inventory in light water reactors." *Nuclear technology* 68.1 (1985): 18-28.

$$^{59}Co + {}^{1}n \longrightarrow {}^{60}Co$$

stable — radioactive

$$\downarrow \; t_{1/2} = 5.27 \text{ years}$$

$$^{60}Ni + \beta^{-} + \gamma$$

stable

1.17 MeV

1.33 MeV

Office for Nuclear Regulation

Office for Nuclear Regulation

An agency of HSE

Report ONR-GDA-AR-11-025
Revision 0

- Choosing materials to reduce activated corrosion products (mainly cobalt isotopes).

4.1.1.4.1 Cobalt Reduction

86 In many nuclear power plants (NPPs), activated corrosion products in the primary coolant increase dose rates through activation of cobalt-59 to cobalt-60 in the Stellite^{TM} content of hard facings, and activation of nickel-58 to cobalt-58 in inconel 690 alloys and some stainless steels; cobalt-58 and cobalt-60 typically account for over 80% of equivalent dose rates associated with the primary coolant.

Office for Nuclear Regulation

360. The other significant usage of Stellite™ in UK ABWR is within valves. Ref. 81 provides information on the different types and locations of valves. The vast majority (>[redacted]) is within the CFDW and MS systems. Hitachi-GE estimates that these valves are the greatest source of cobalt release into the coolant of UK ABWR, accounting for around [redacted] (again, noting that I consider that this is potentially underestimated due to wear releases). Hitachi-GE's approach is that the choice of valve seat hard facing material is based on multiple factors such as size, nuclear safety significance, location, fluid property, fluid temperature, valve type and frequency of use. It is widely acknowledged, including by Hitachi-GE that cobalt-base hard facing materials generally offer superior performance and reliability compared to nickel- or iron-base alternatives. This is a reasonable starting point for reviewing if further reductions are possible.

** Same group as Kim & Kim*

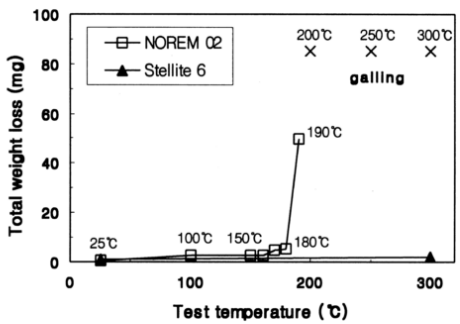

Kim & Kim, Wear 237 (2000)
Button-on-block in air

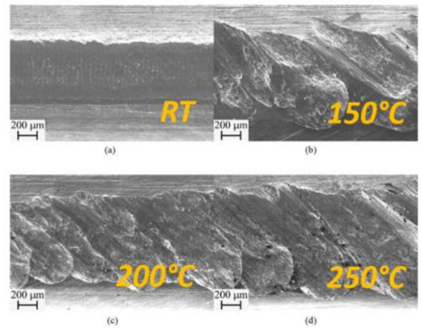

Persson et al., Wear 255 (2003)
Linear sliding in air

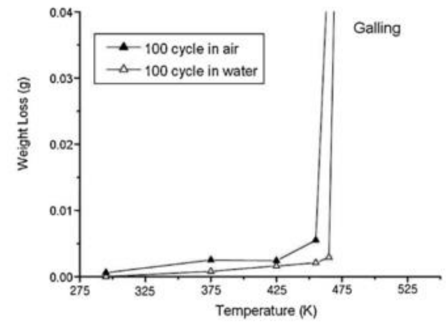

Lee et al.*, Wear 262 (2007)
Button-on-block in air and in pressurised water NOT PWR chemistry

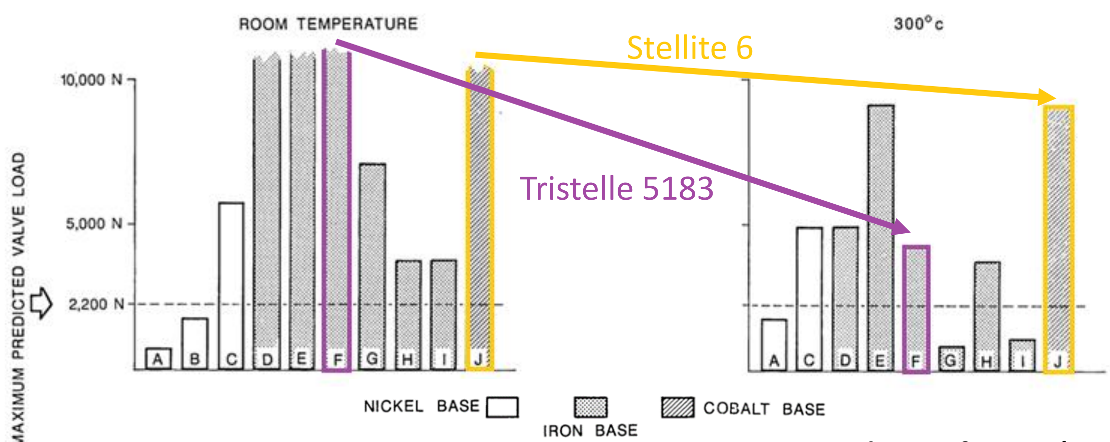

Burdett, Surf. Eng. 8 (1992)
Button-on-block in air

Why do iron-based hard-facings fail at elevated temperature?

Technique 1: A very brief introduction to EBSD

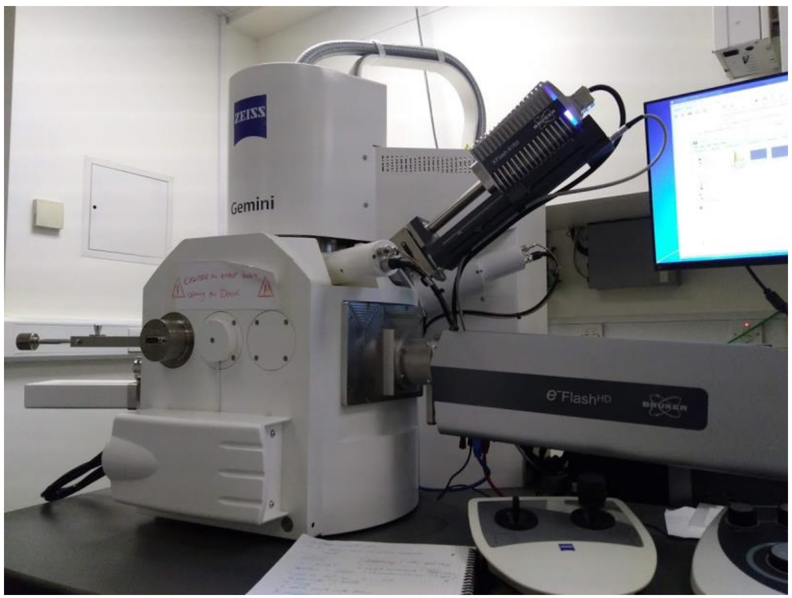

My colleagues: Zeiss Sigma 300 & Bruker e-flash HD

- **E**lectron **b**ack**s**catter **d**iffraction

- Gives rich microstructural maps full of…
  - Orientations
  - Grains – shapes, size (distributions)

- With a bit more care we can measure…
  - Strains
  - Dislocations densities

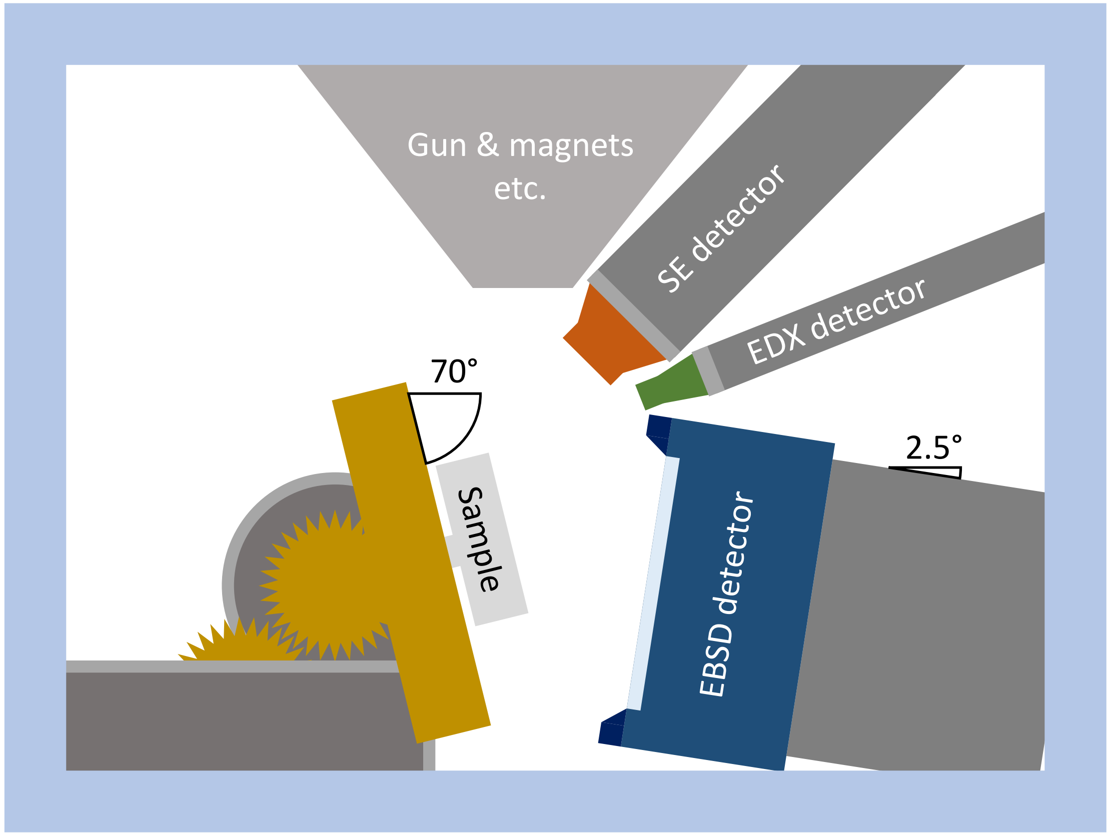

Inside the scanning electron microscope

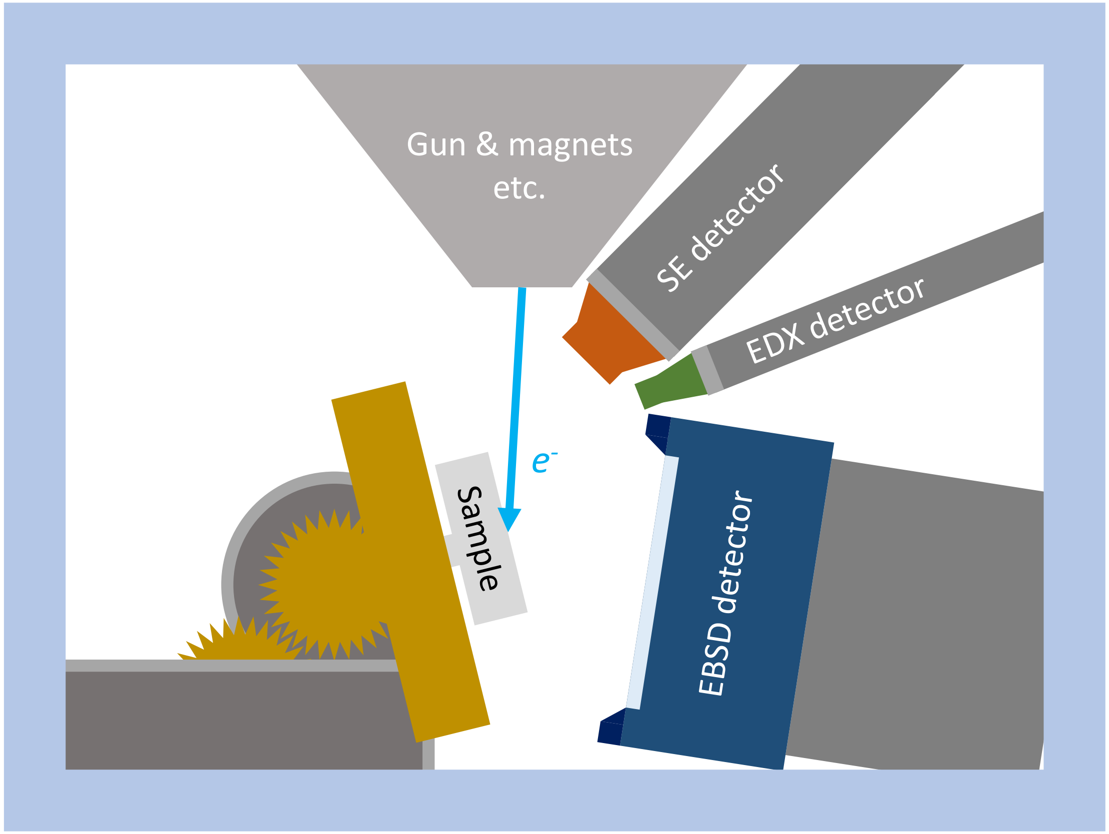
Gun & magnets
etc.
SE detector
EDX detector
e^-
Sample
EBSD detector

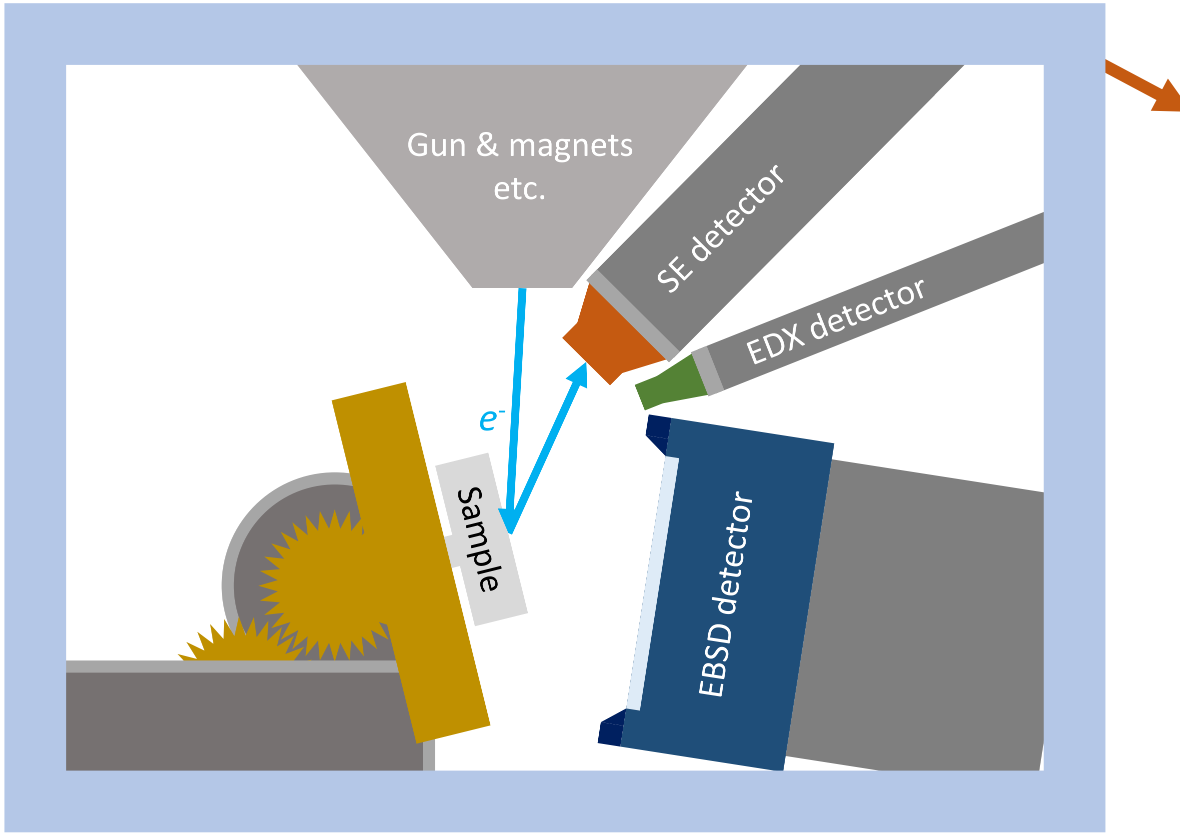

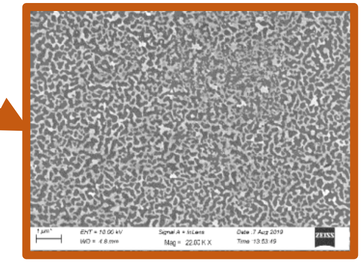

Normal imaging
(secondary electron)

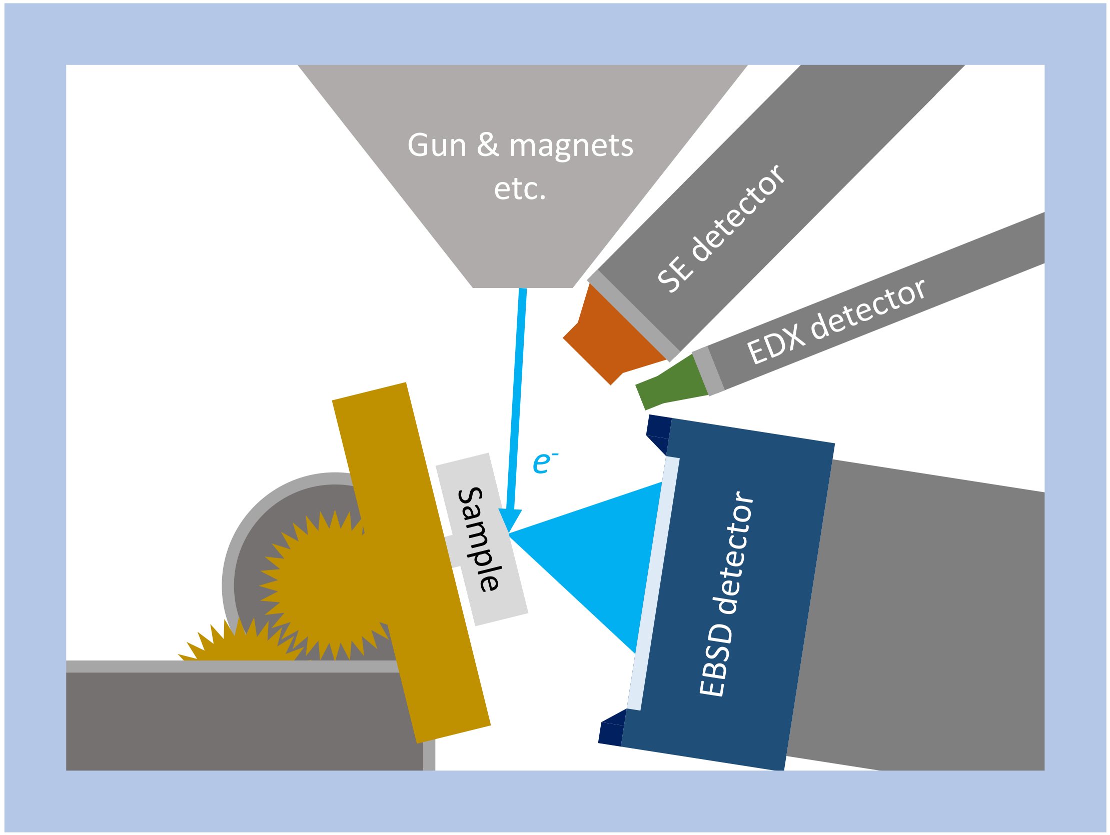
Gun & magnets etc.
SE detector
EDX detector
e^-
Sample
EBSD detector

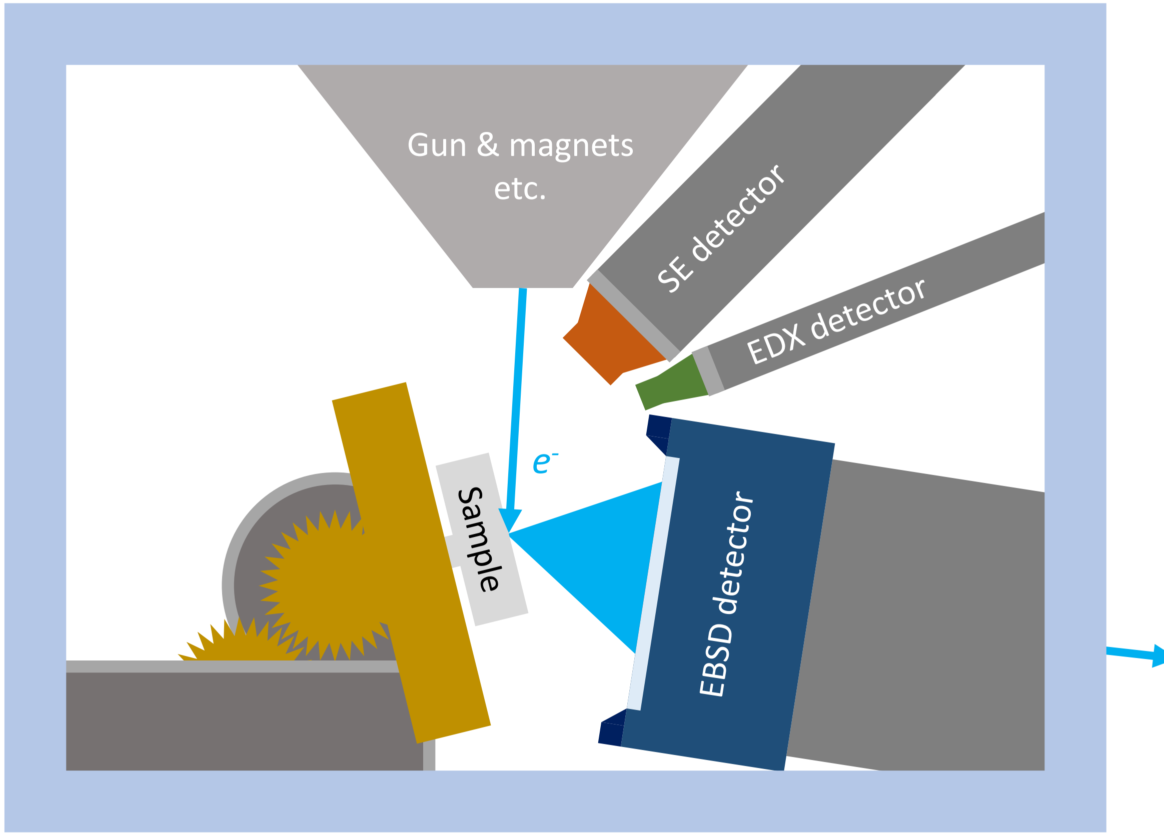

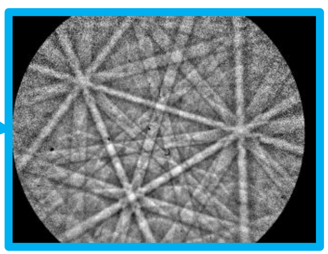

Electron
backscatter
diffraction pattern

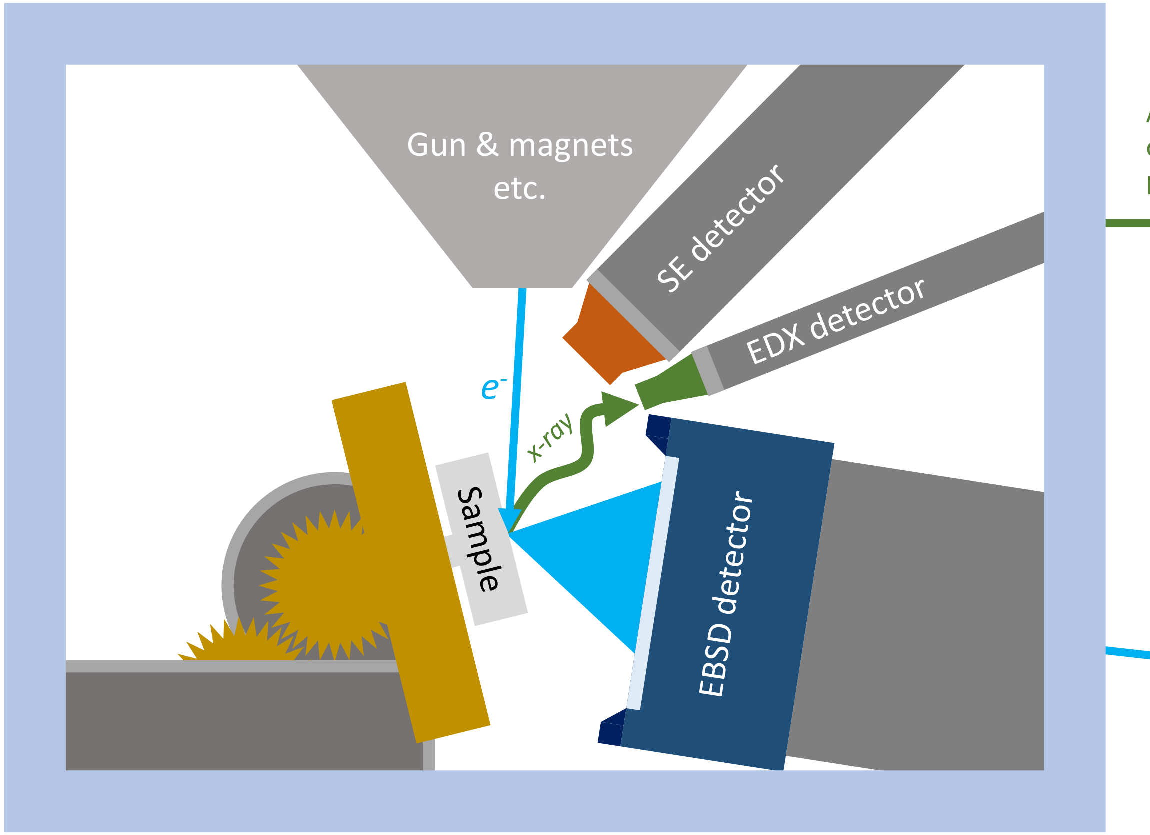

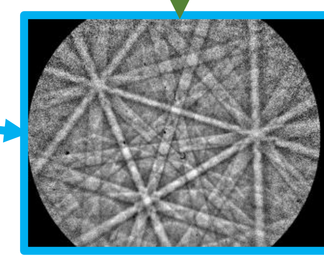

Electron
backscatter
diffraction pattern

Standard EBSD

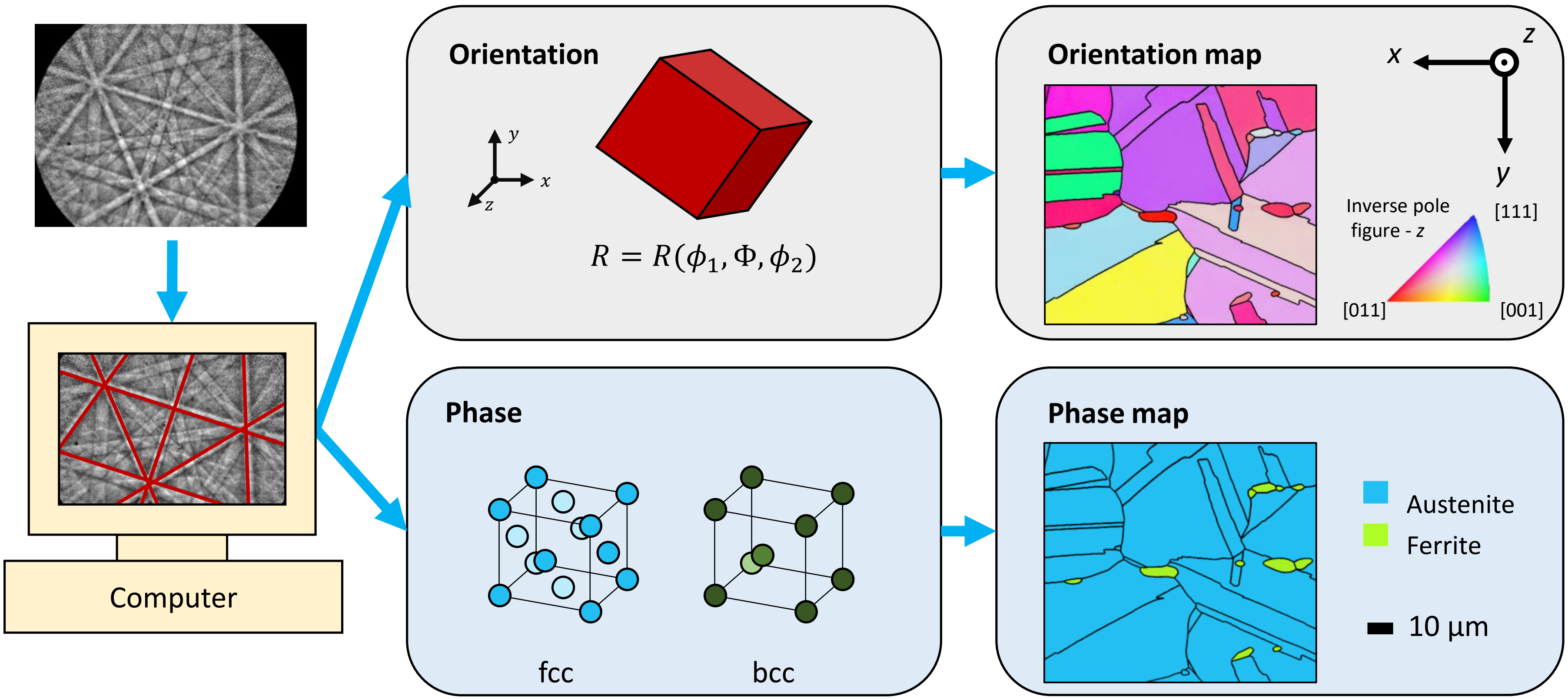

High-angular resolution EBSD

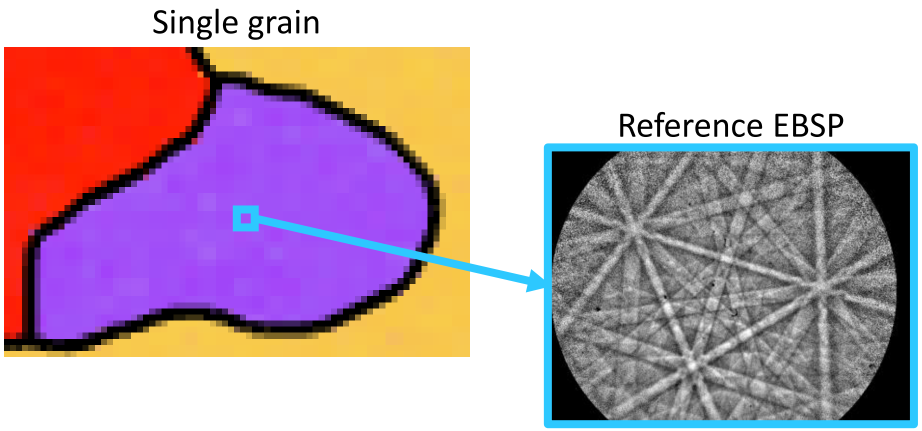

Wilkinson, Angus J., Graham Meaden, and David J. Dingley. "High resolution mapping of strains and rotations using electron backscatter diffraction." *Materials Science and Technology* 22.11 (**2006**): 1271-1278.

High-angular resolution EBSD

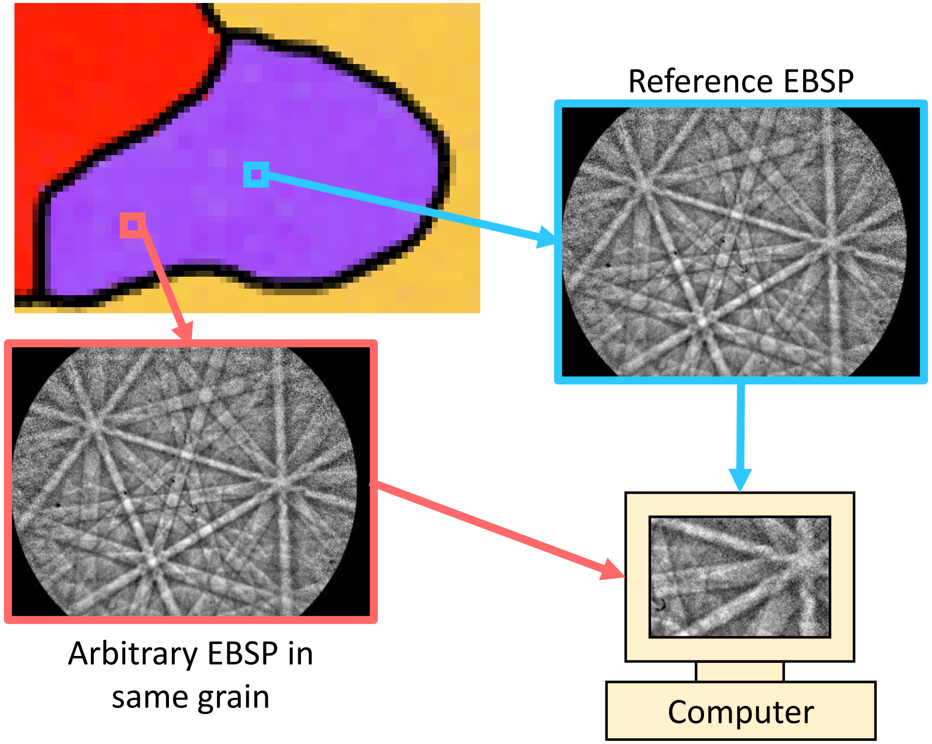

Britton, T. B., and Angus J. Wilkinson. "High resolution electron backscatter diffraction measurements of elastic strain variations in the presence of larger lattice rotations." Ultramicroscopy 114 (2012): 82-95.

High-angular resolution EBSD

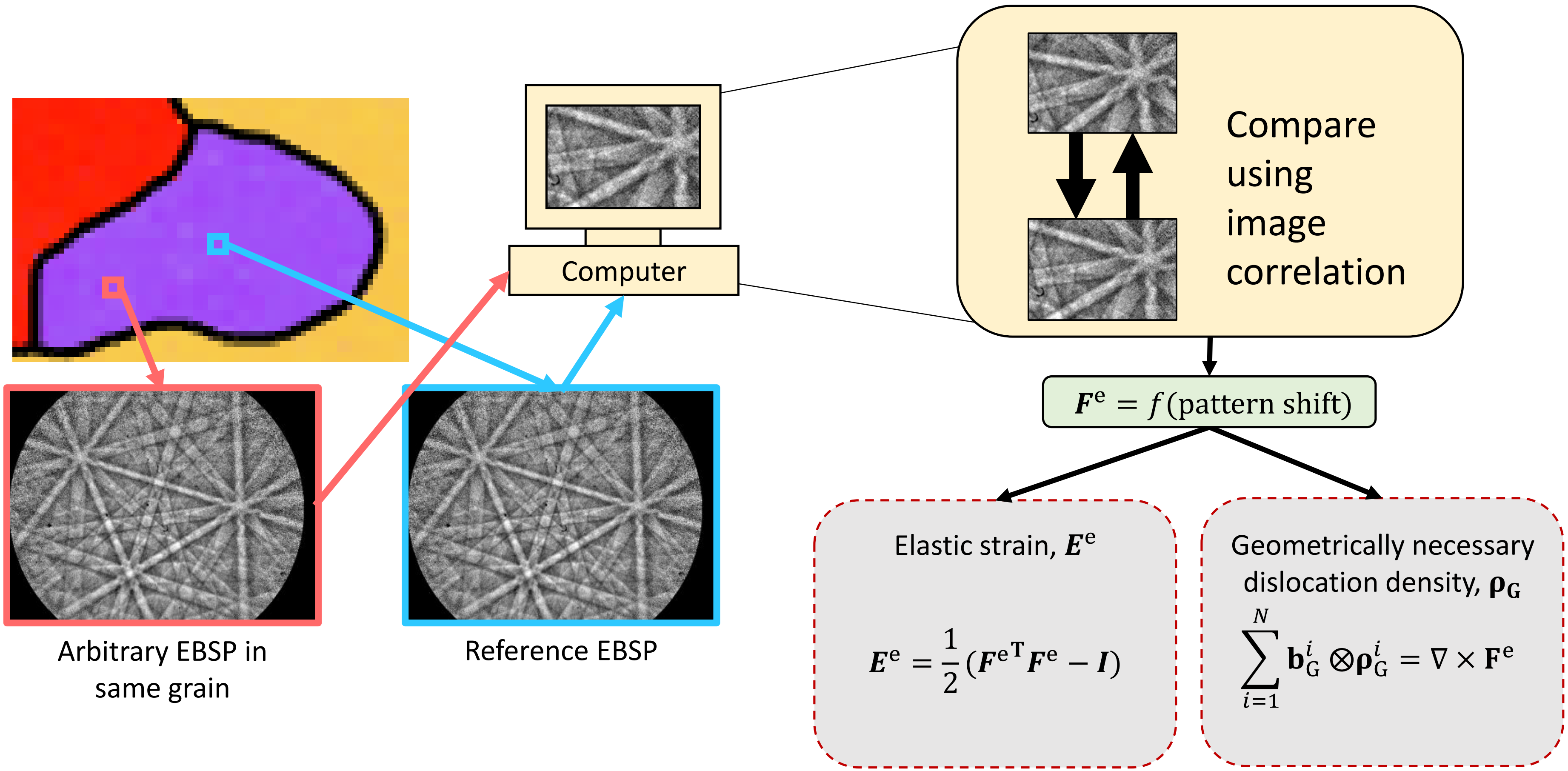

Technique 2: A very quick introduction to DIC

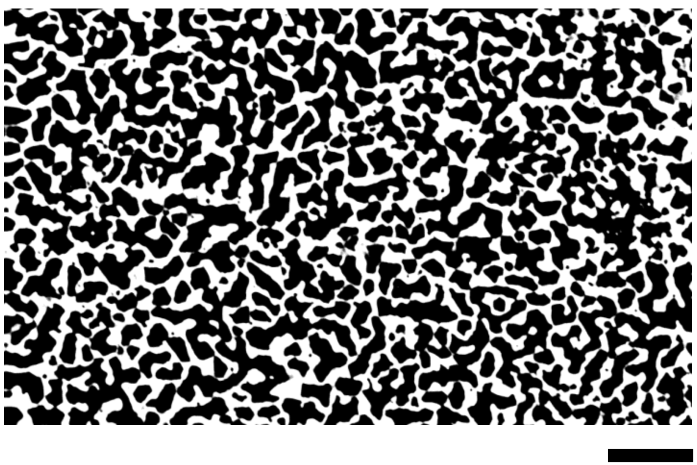

- **D**igital **i**mage **c**orrelation
- Pattern sample
- Track motion of pattern
- Calculate strains/rotations

Technique 2: A very quick introduction to DIC

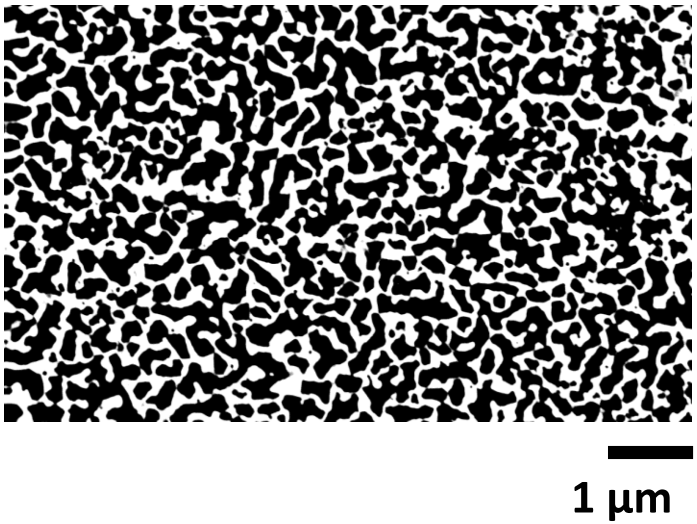

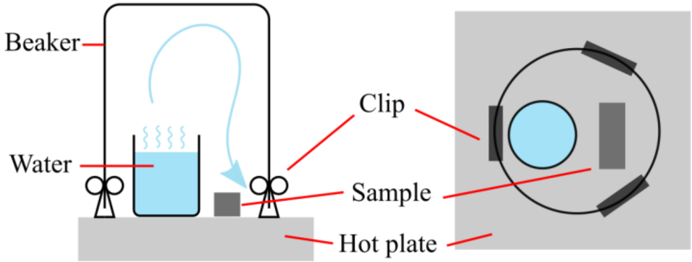

(a) Side view (b) Top view

(c) Photograph

Scrivens, W. A., et al. "Development of patterns for digital image correlation measurements at reduced length scales." *Experimental Mechanics* 47.1 (2007): 63-77.

Pre- and post-deformation images

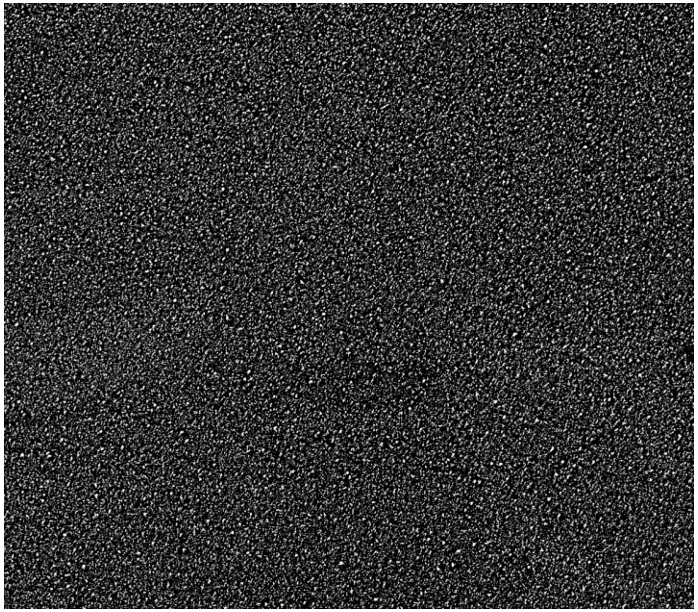

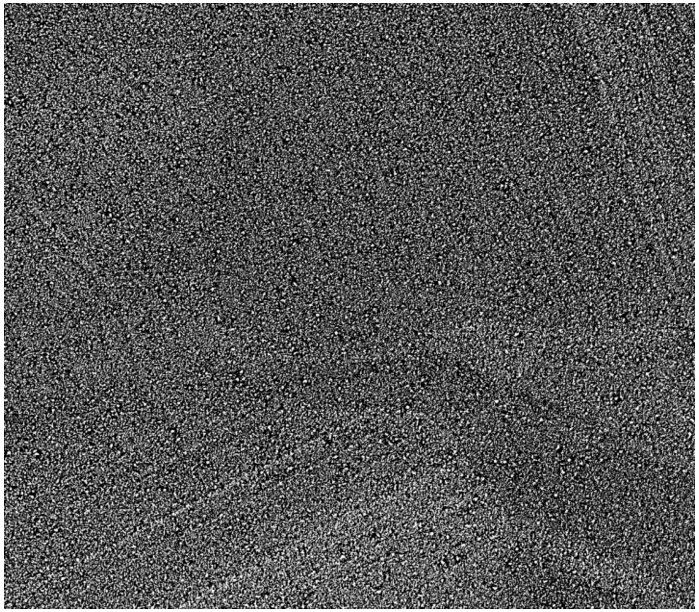

We need features in both images

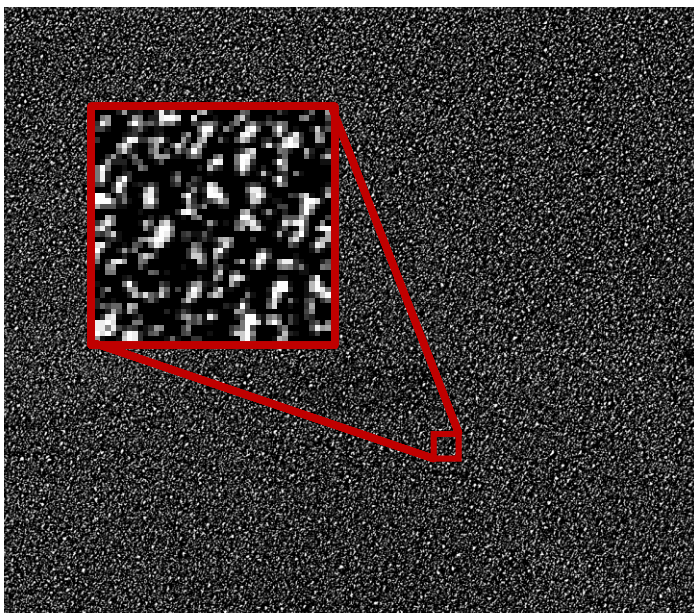

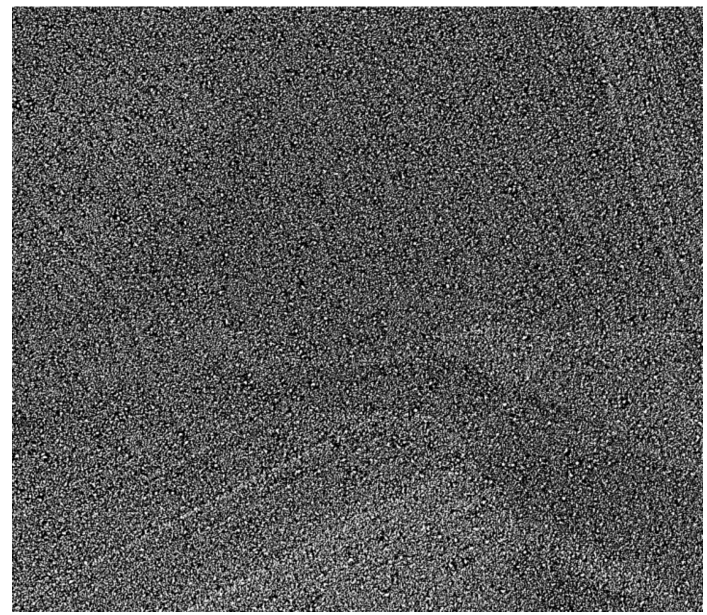

We need features in both images

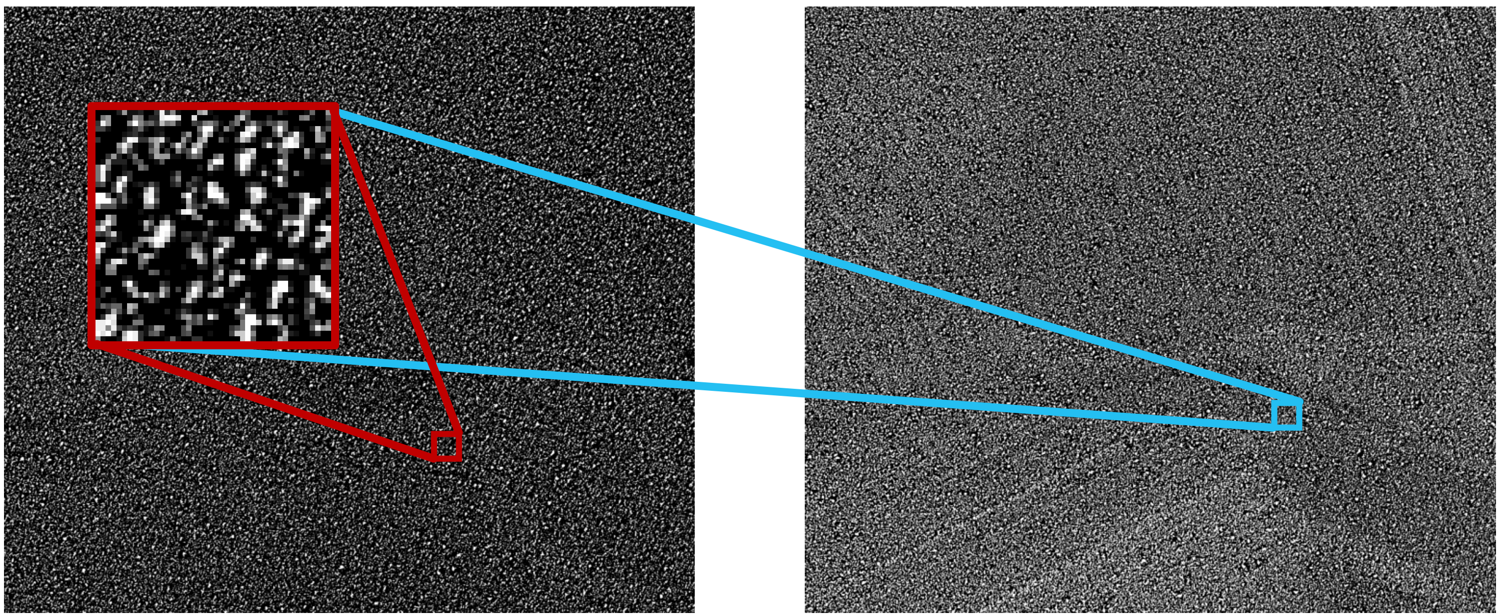

Compare and calculate shifts

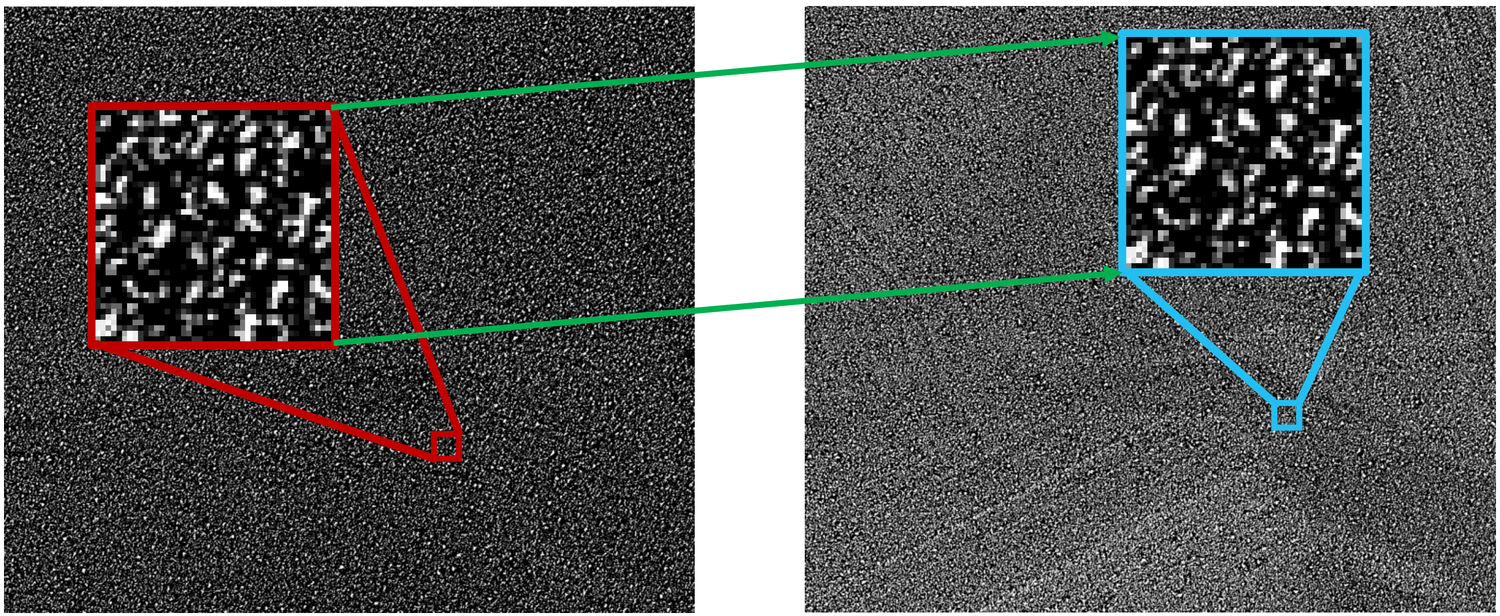

Convert the shifts into strain

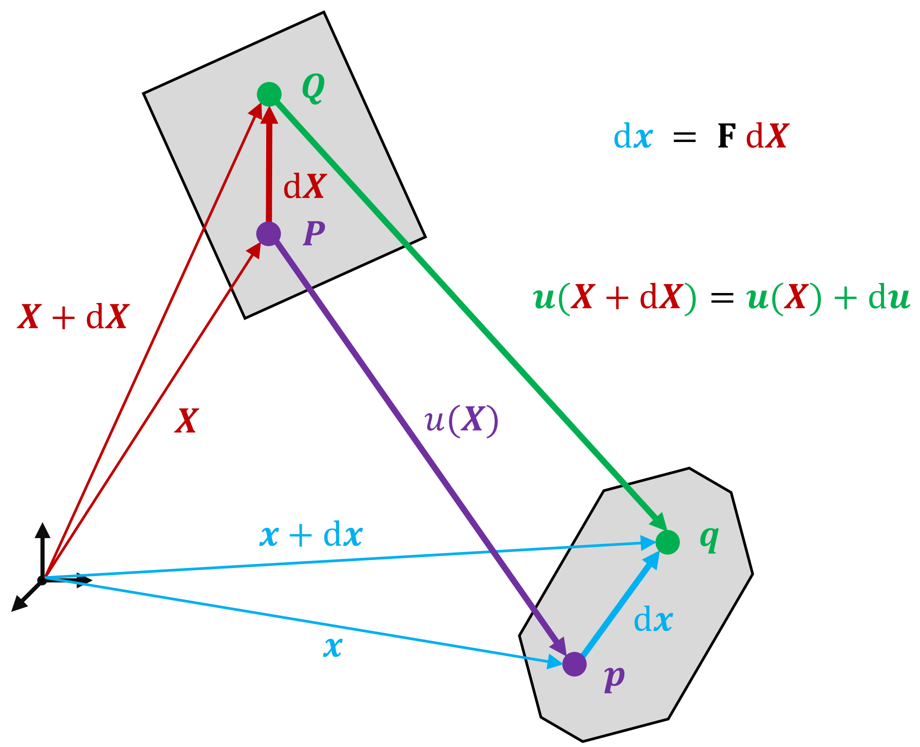

$$\boldsymbol{F} = \begin{pmatrix} F_{11} & F_{12} & F_{13} \\ F_{21} & F_{22} & F_{23} \\ F_{31} & F_{32} & F_{33} \end{pmatrix}$$

$$\boldsymbol{F} = \begin{pmatrix} F_{11} & F_{12} & ? \\ F_{21} & F_{22} & ? \\ ? & ? & ? \end{pmatrix}$$

Total strain, $\boldsymbol{E}$

$$\boldsymbol{E} = \frac{1}{2}(\boldsymbol{F}^{\mathrm{T}}\boldsymbol{F} - \boldsymbol{I})$$

Effective strain, E_{eff}

$$E_{\mathrm{eff}} = \sqrt{\frac{2}{3}\boldsymbol{E}:\boldsymbol{E}}$$

Recapitulation

HR-EBSD	HR-DIC
• Ex-situ • Elastic residual strains - $\boldsymbol{E}^{\mathrm{e}}$ • Geometrically necessary dislocation density - ρ_G	• Ex-situ • Total strains - $\boldsymbol{E}$

Loading conditions

Specimen for small scale three point bend

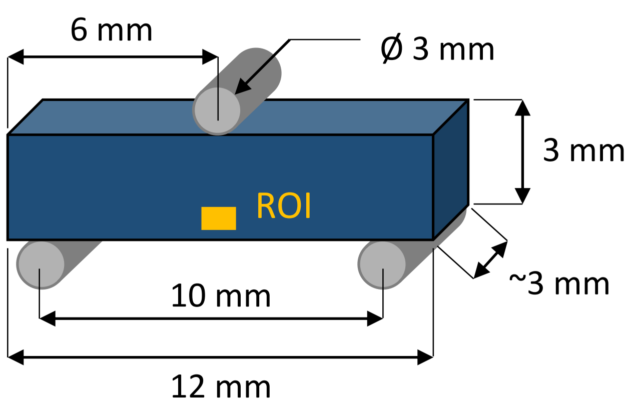

Force and temperature loading conditions

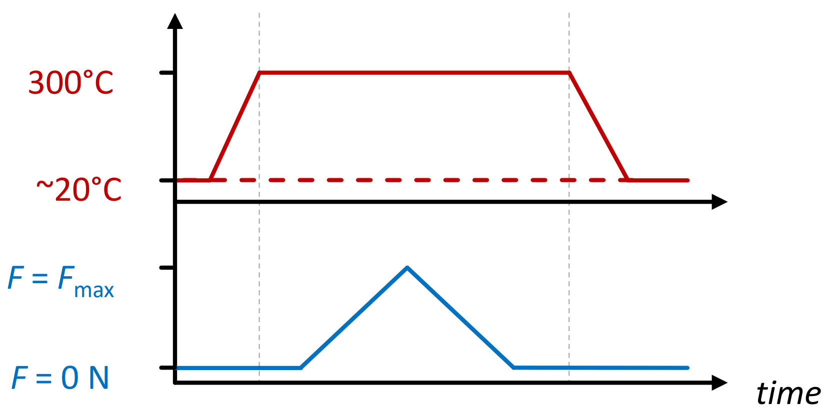

Bending hot pieces of metal

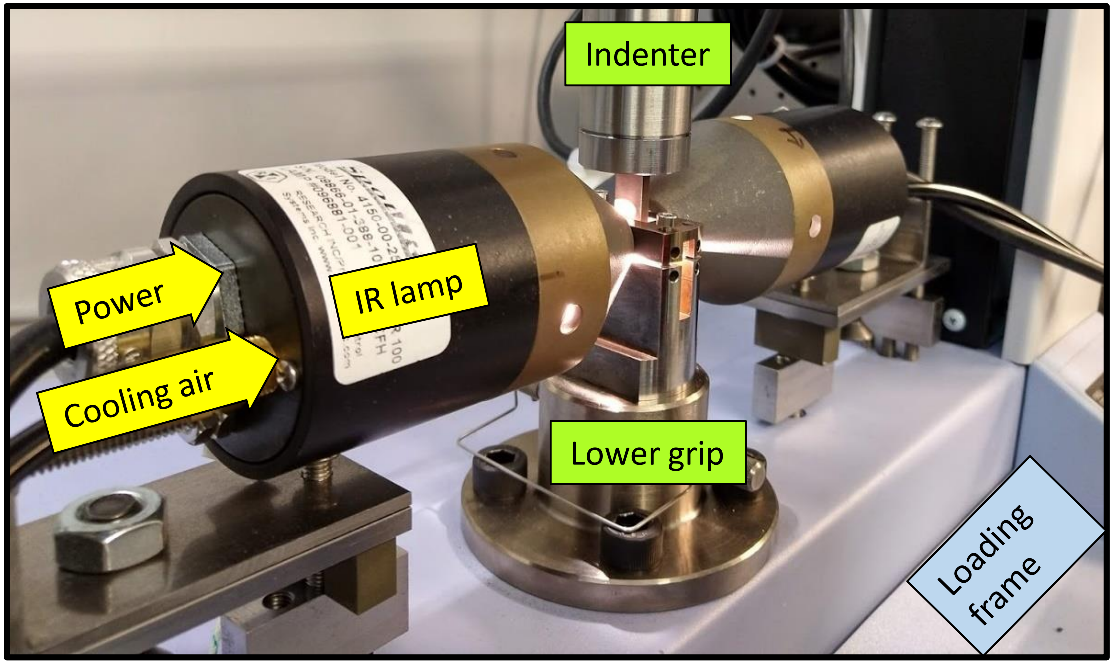

Bending hot pieces of metal

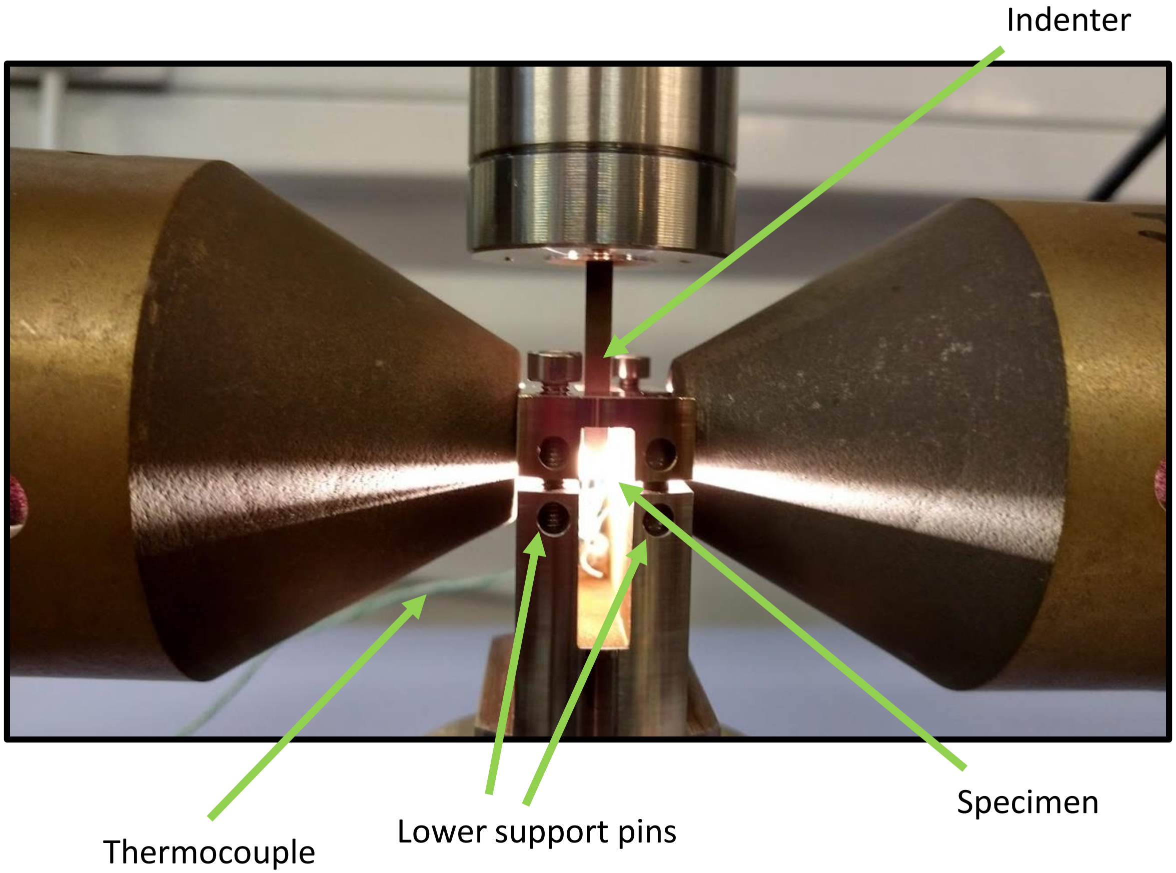

Experimental workflow

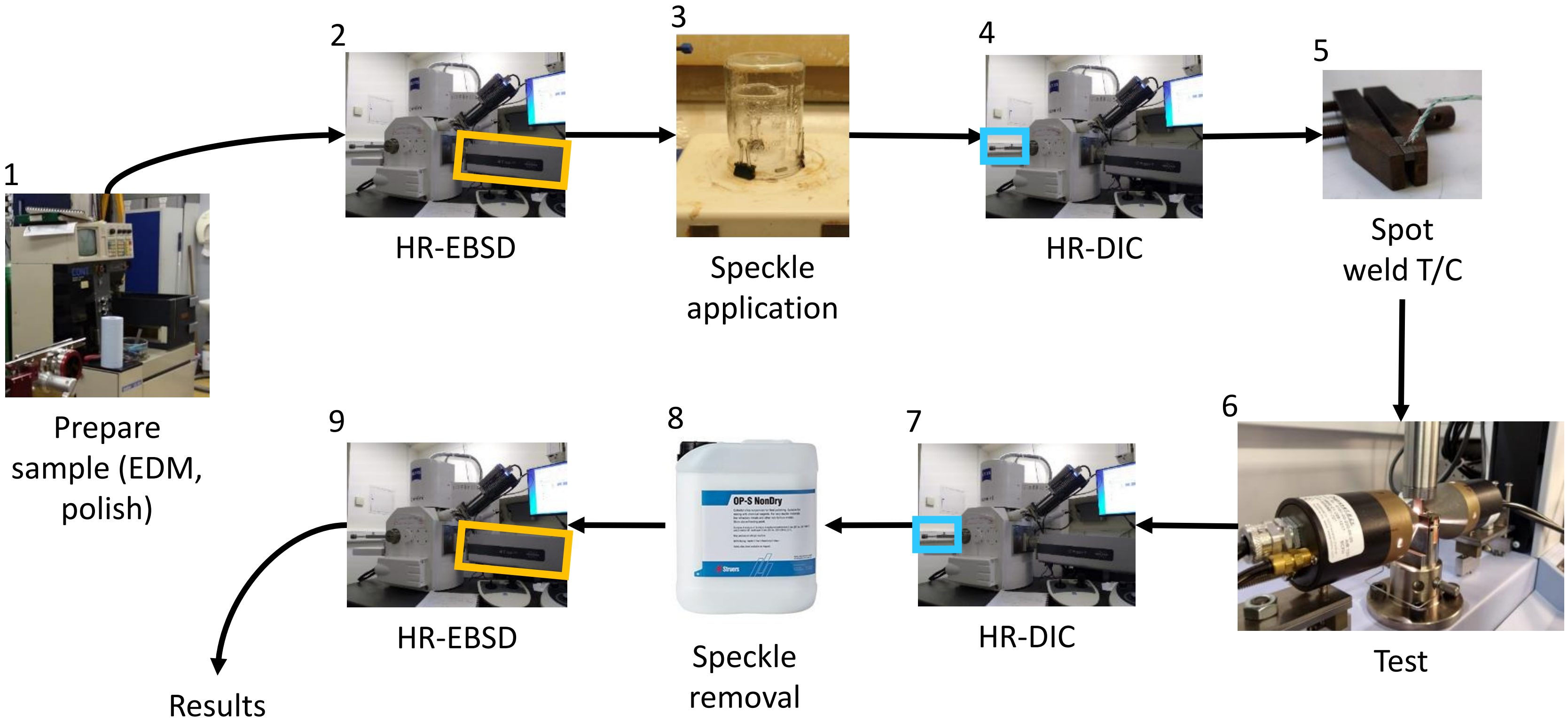

Materials

Austenite
Ferrite
Niobium carbide
Chromium carbide (7/3)

Nitronic 60 - Cast and extruded rod

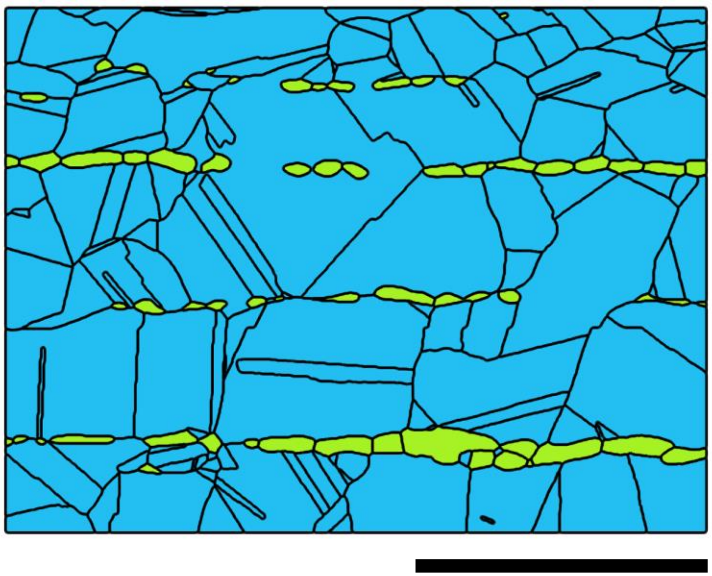

Tristelle 5183 – Powder HIPed

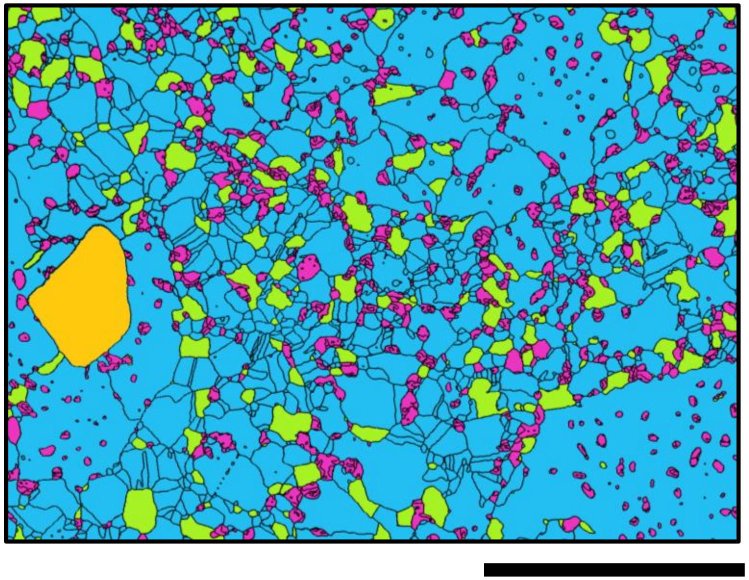

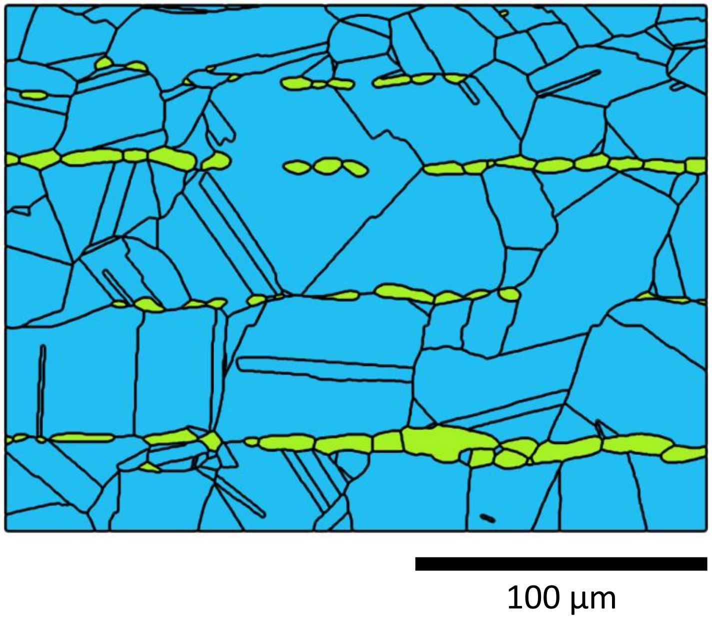

Nitronic 60

A simple microstructure with simple micromechanics?

Room temperature

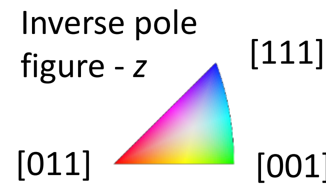

Phase map

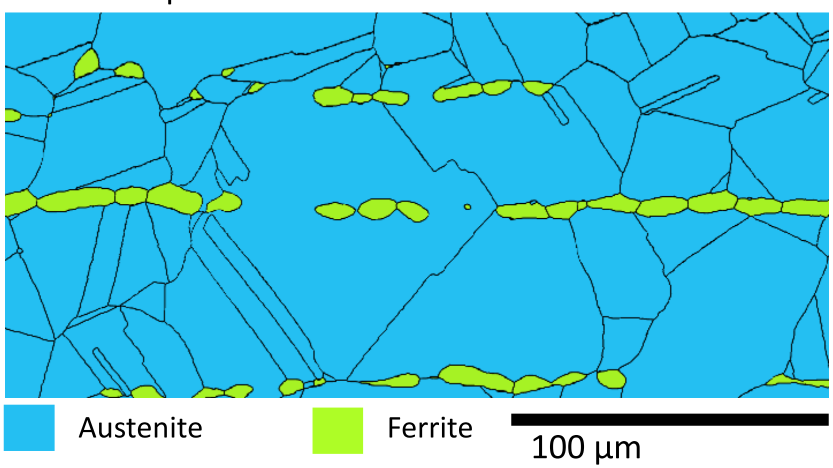

Orientation map

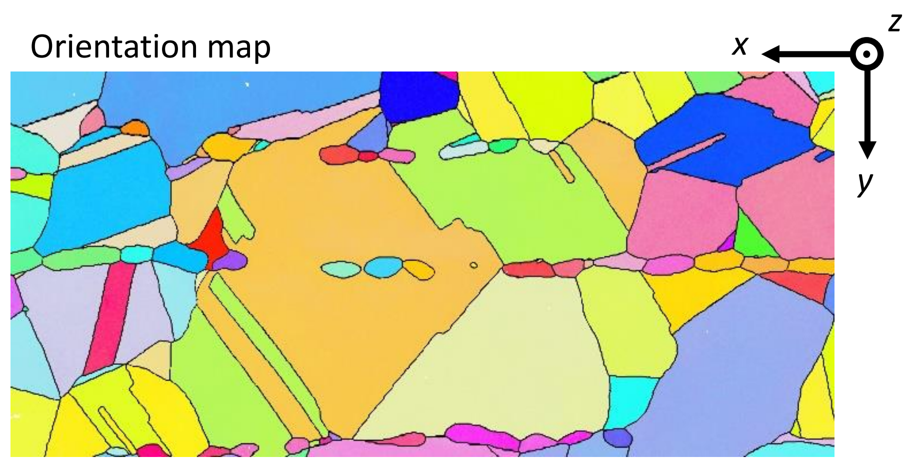

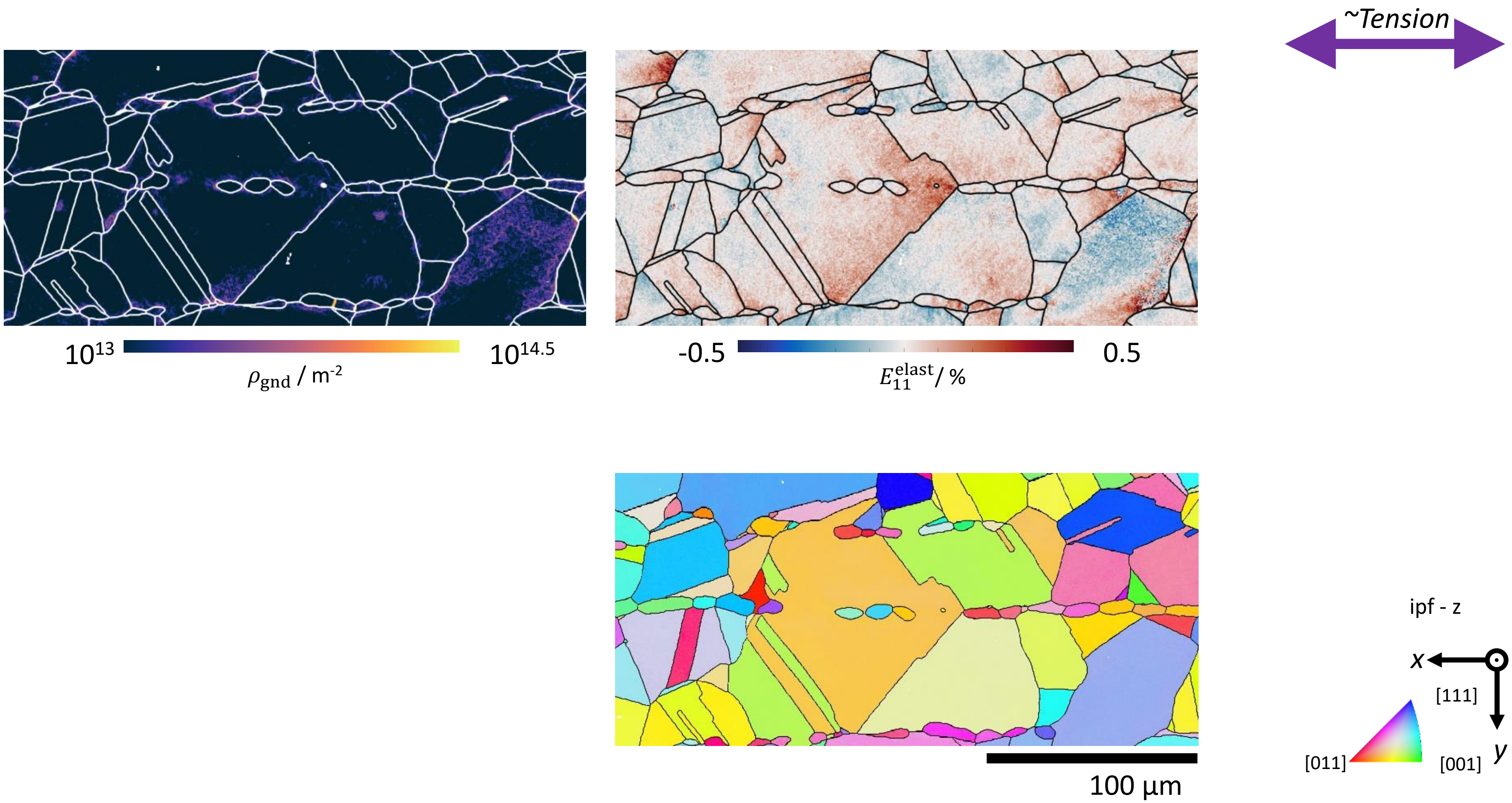
~Tension
10^{13}
$10^{14.5}$
ρ_{gnd} / m^{-2}
-0.5
0.5
E_{11}^{elast} / %
100 µm
ipf - z
x
z
y
[111]
[011]
[001]

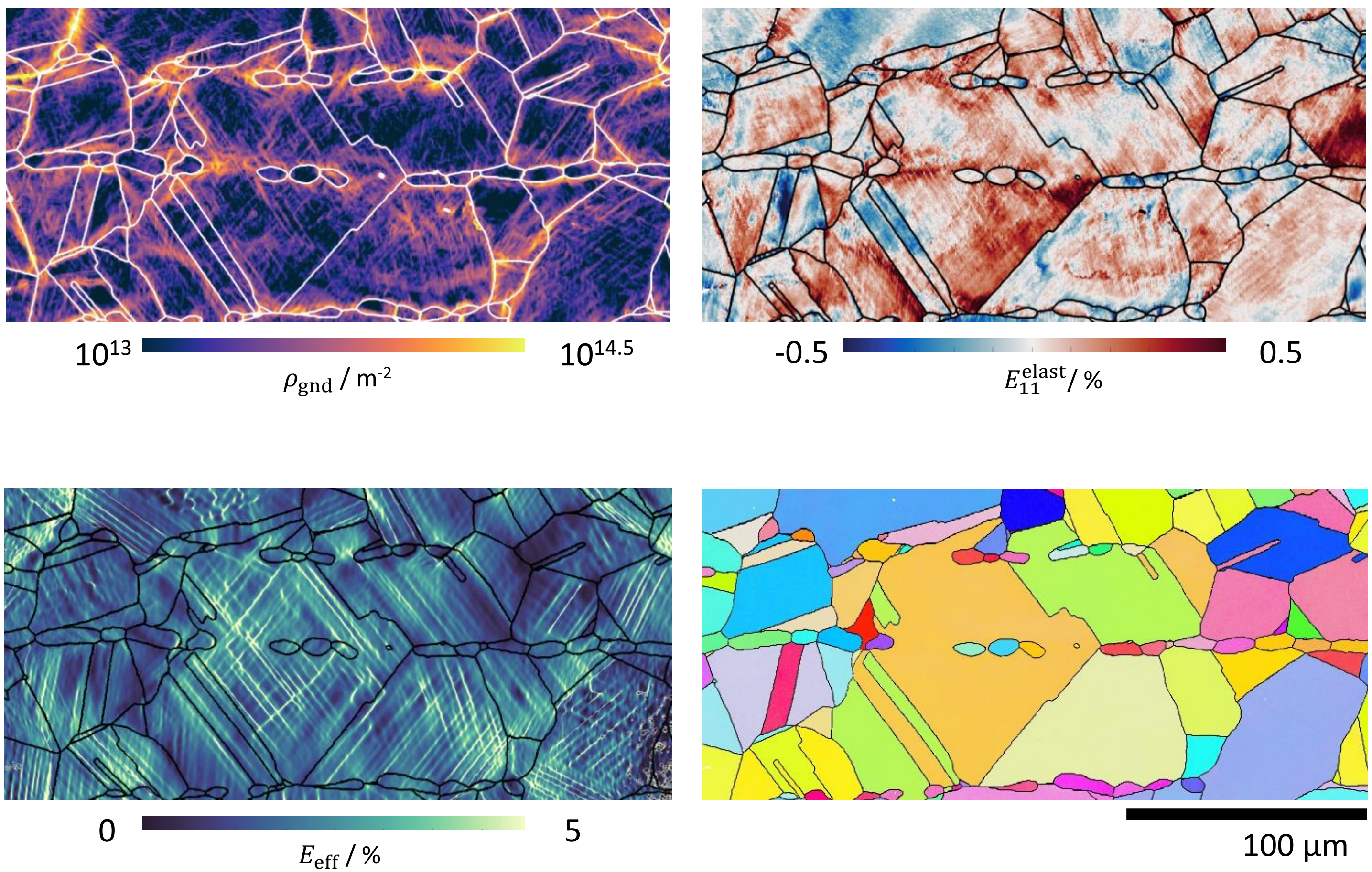

*The apparent drift is due to extremely long (~15 h) EBSD scnas

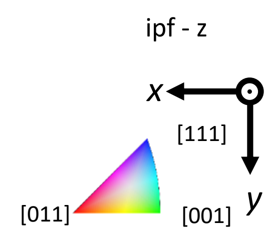

300°C - specimen 1

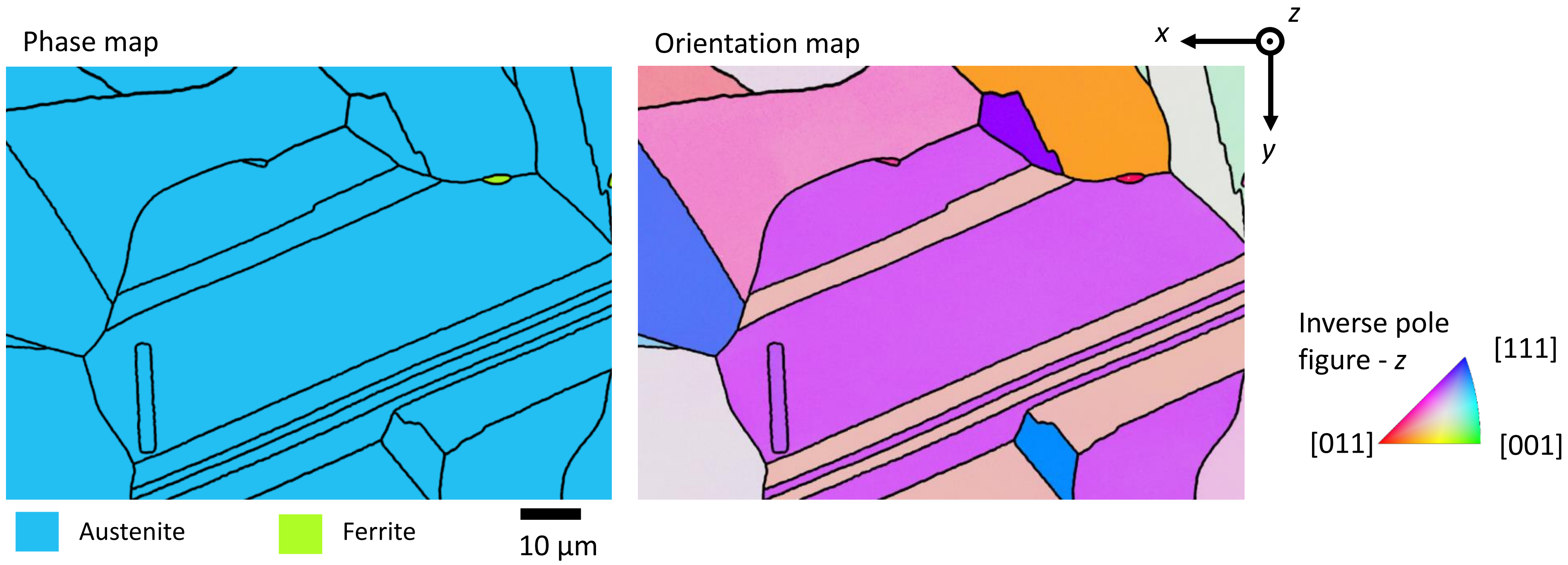

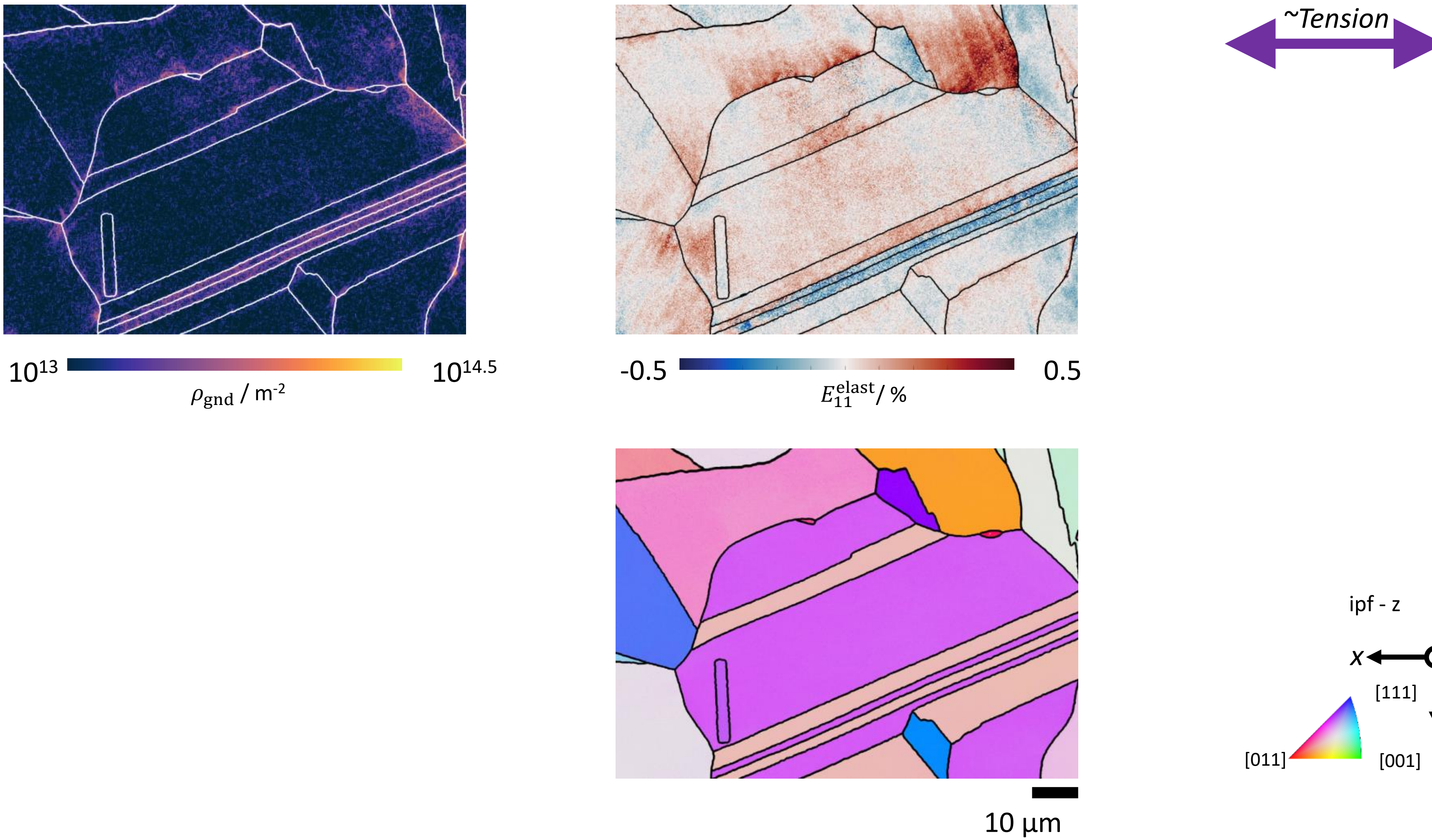

~Tension
10^{13}
$10^{14.5}$
ρ_{gnd} / m^{-2}
-0.5
0.5
E_{11}^{elast} / %
ipf - z
x
z
y
[111]
[011]
[001]
10 µm

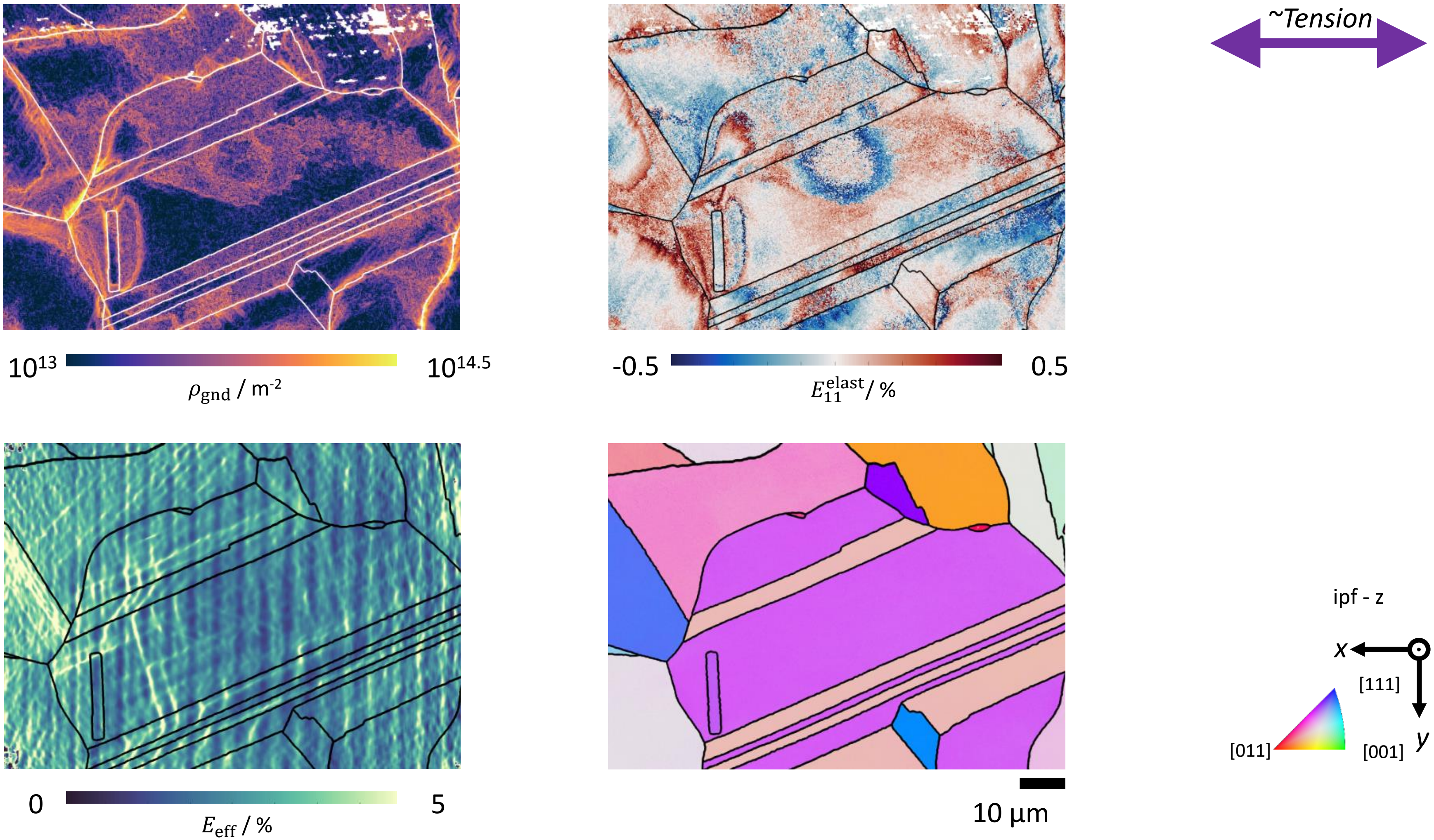

~Tension
10^{13}
$10^{14.5}$
ρ_{gnd} / m^{-2}
-0.5
0.5
E_{11}^{elast} / %
0
5
E_{eff} / %
10 µm
ipf - z
x
z
y
[111]
[011]
[001]

300°C - sample 2

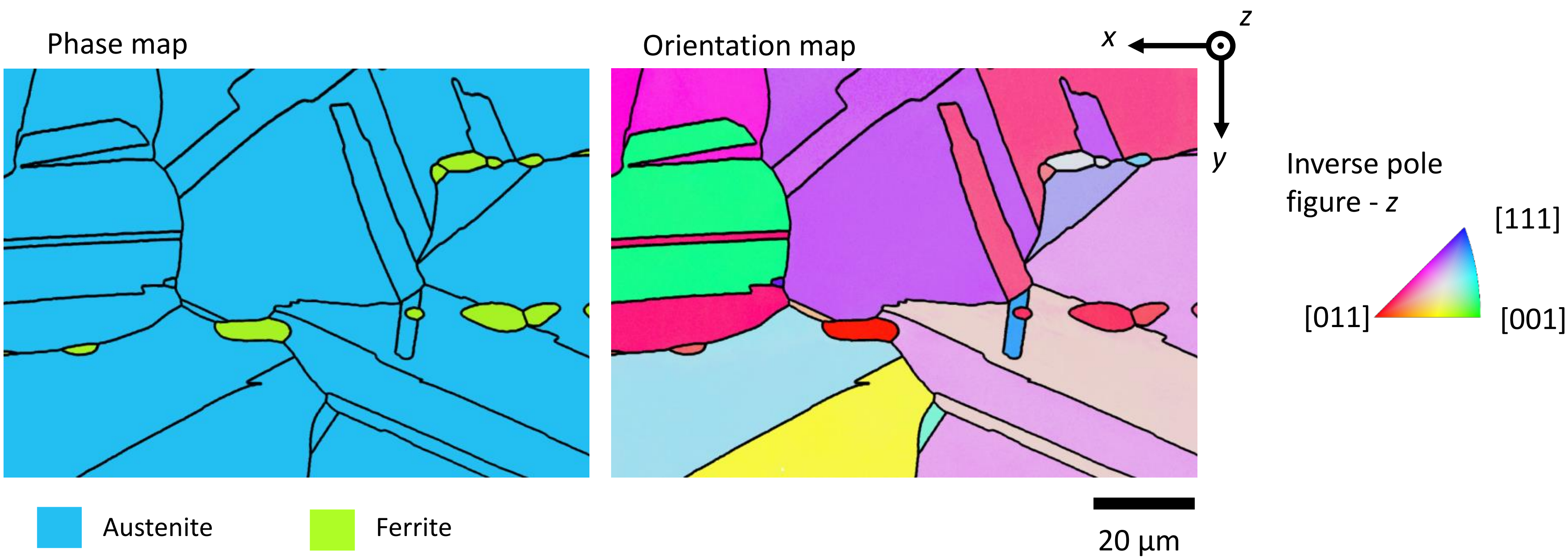

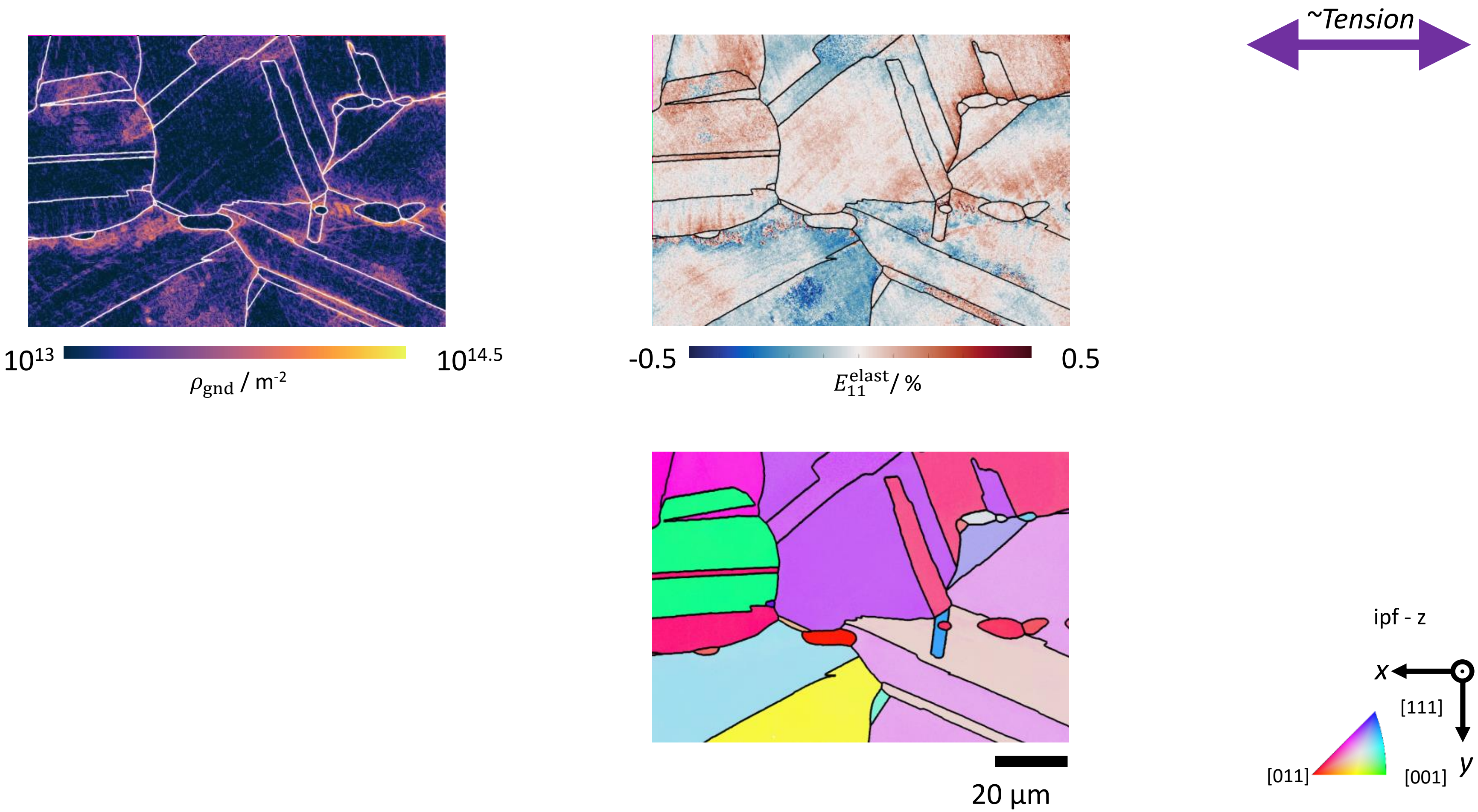
~Tension
10^13
10^14.5
ρ_gnd / m^-2
-0.5
0.5
E_11^elast / %
20 µm
ipf - z
x
y
z
[111]
[011]
[001]

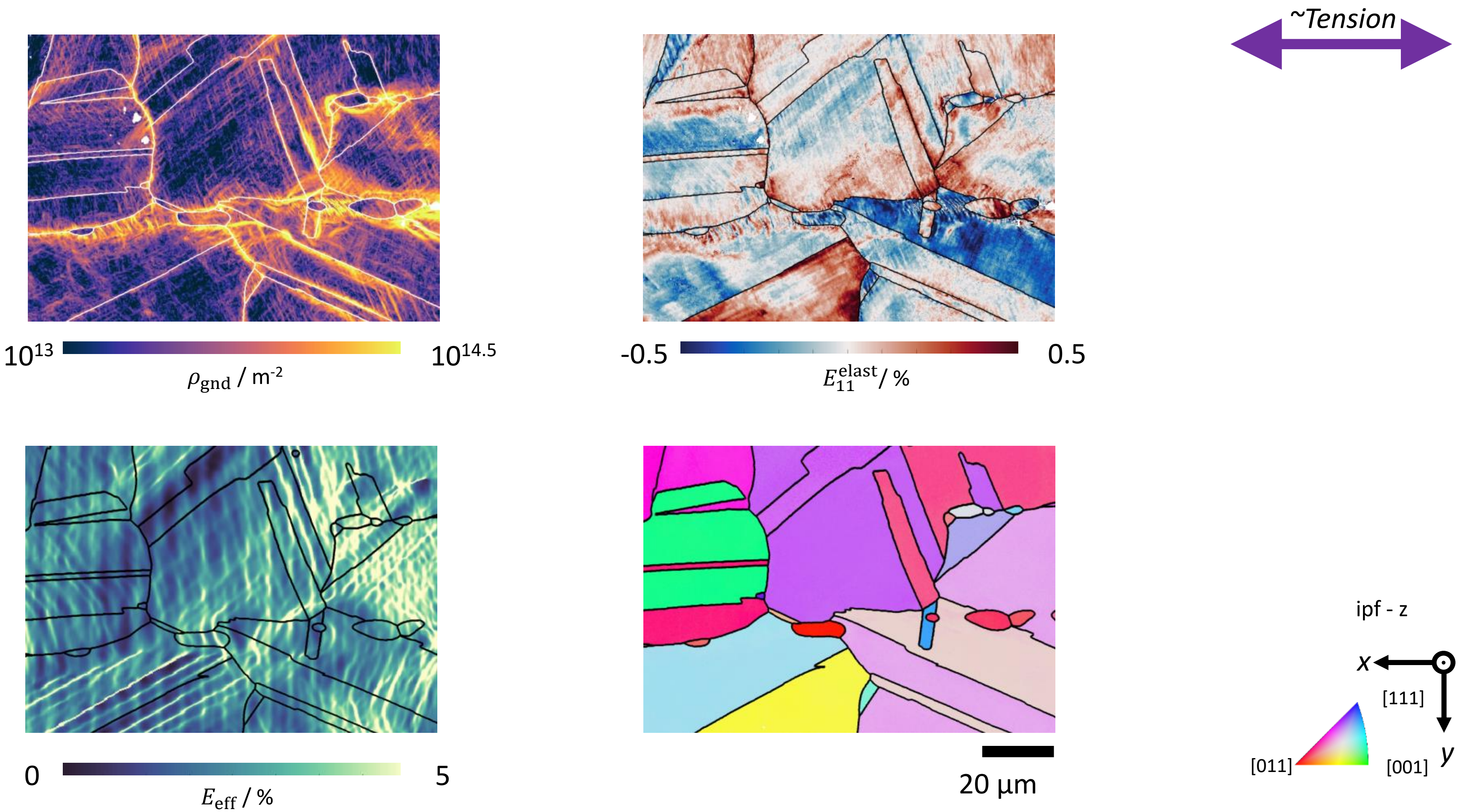
~Tension
10^{13}
$10^{14.5}$
ρ_{gnd} / m^{-2}
-0.5
0.5
E_{11}^{elast} / %
0
5
E_{eff} / %
20 µm
ipf - z
x
y
z
[111]
[011]
[001]

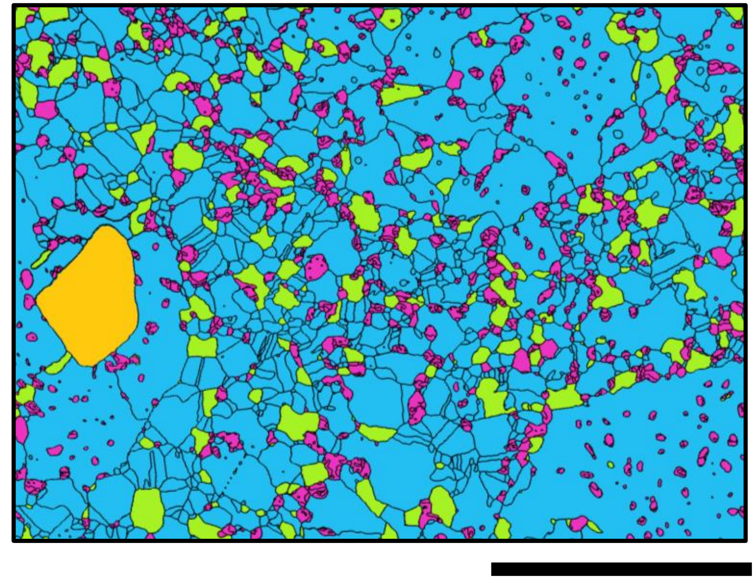

Tristelle 5183

Something a bit more complicated…

Tristelle 5183 – 300°C

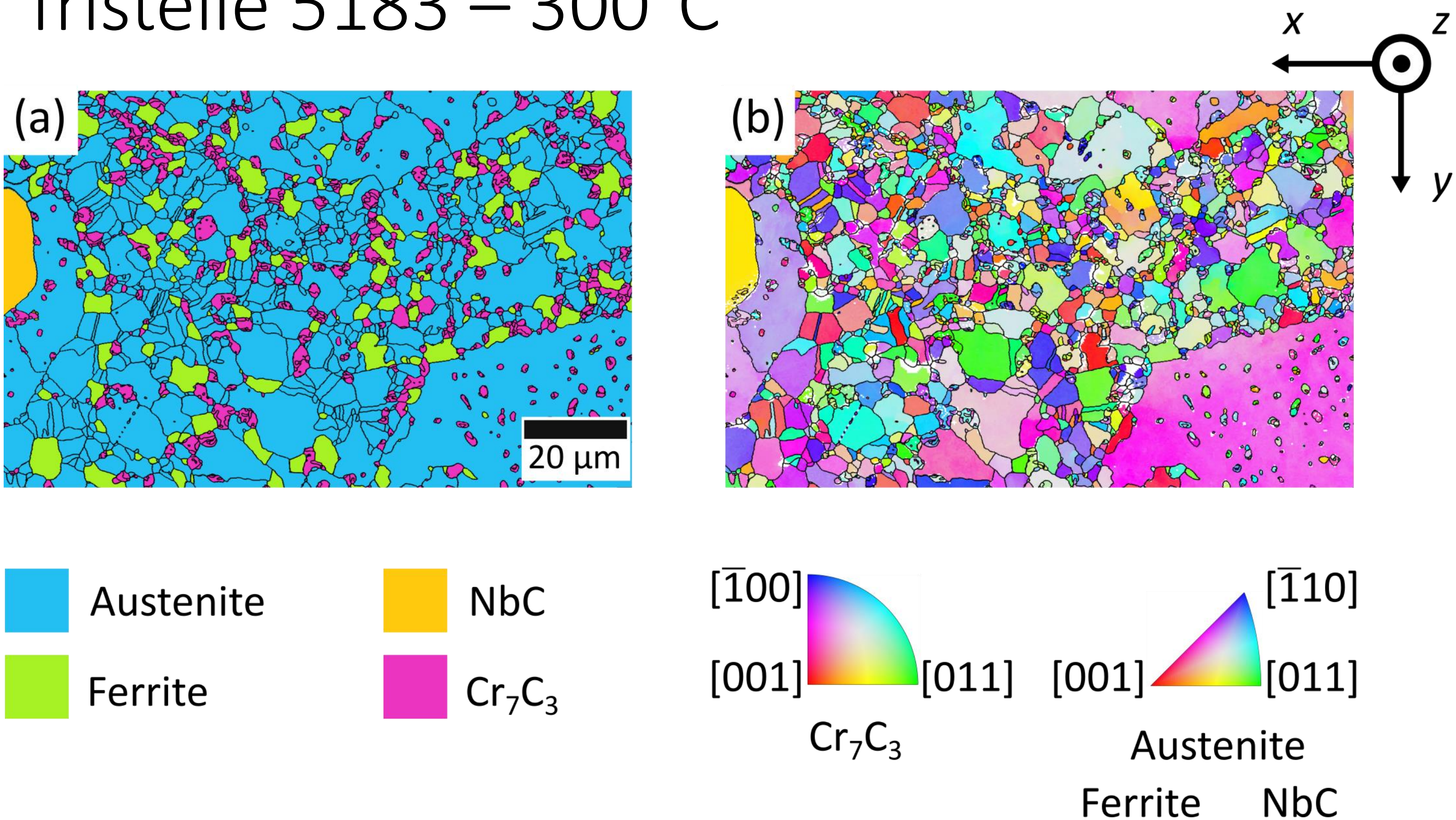

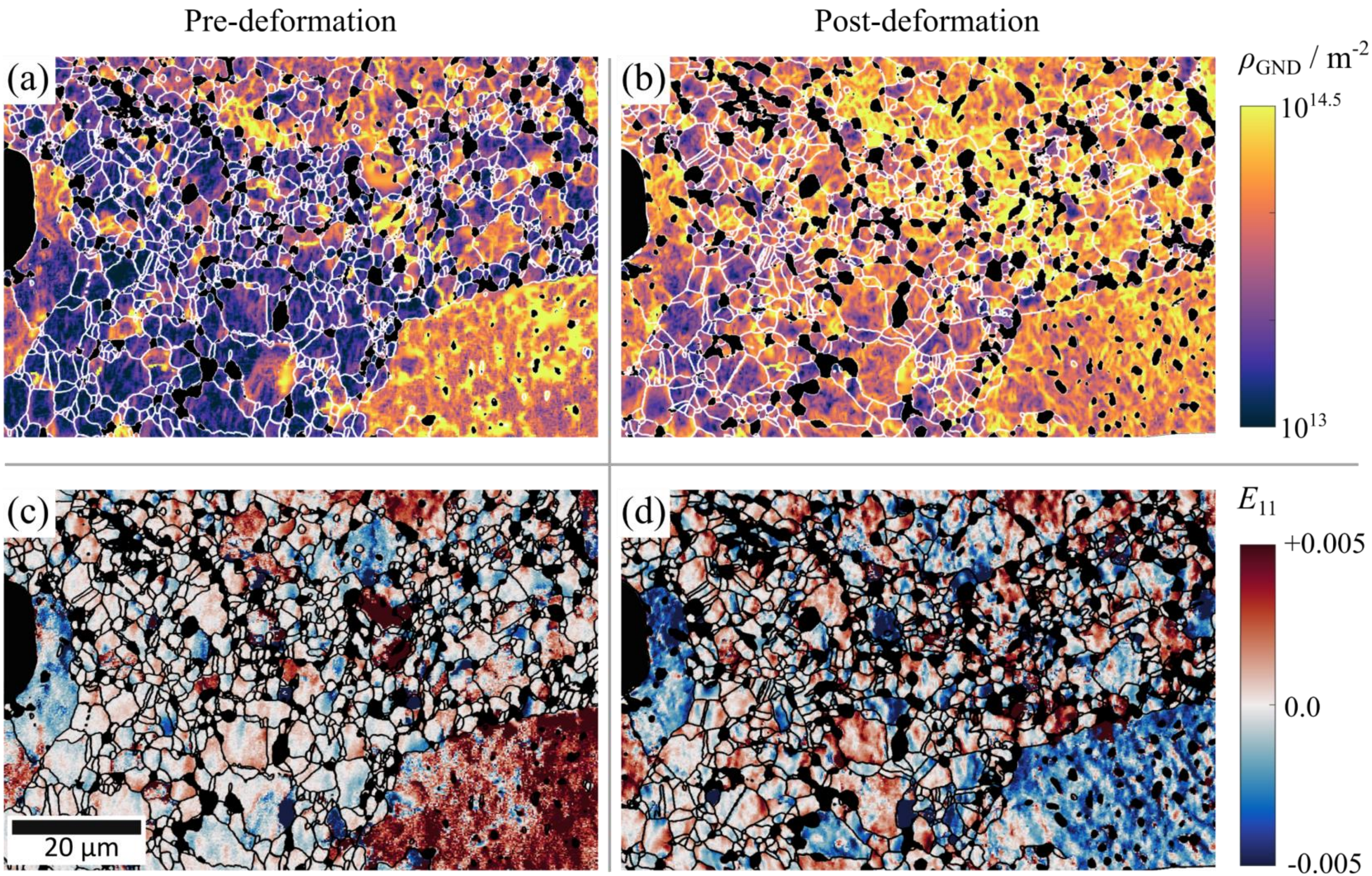

Pre-deformation
Post-deformation
(a)
(b)
(c)
(d)
ρ_{GND} / m^{-2}
$10^{14.5}$
10^{13}
E_{11}
+0.005
0.0
-0.005
20 µm

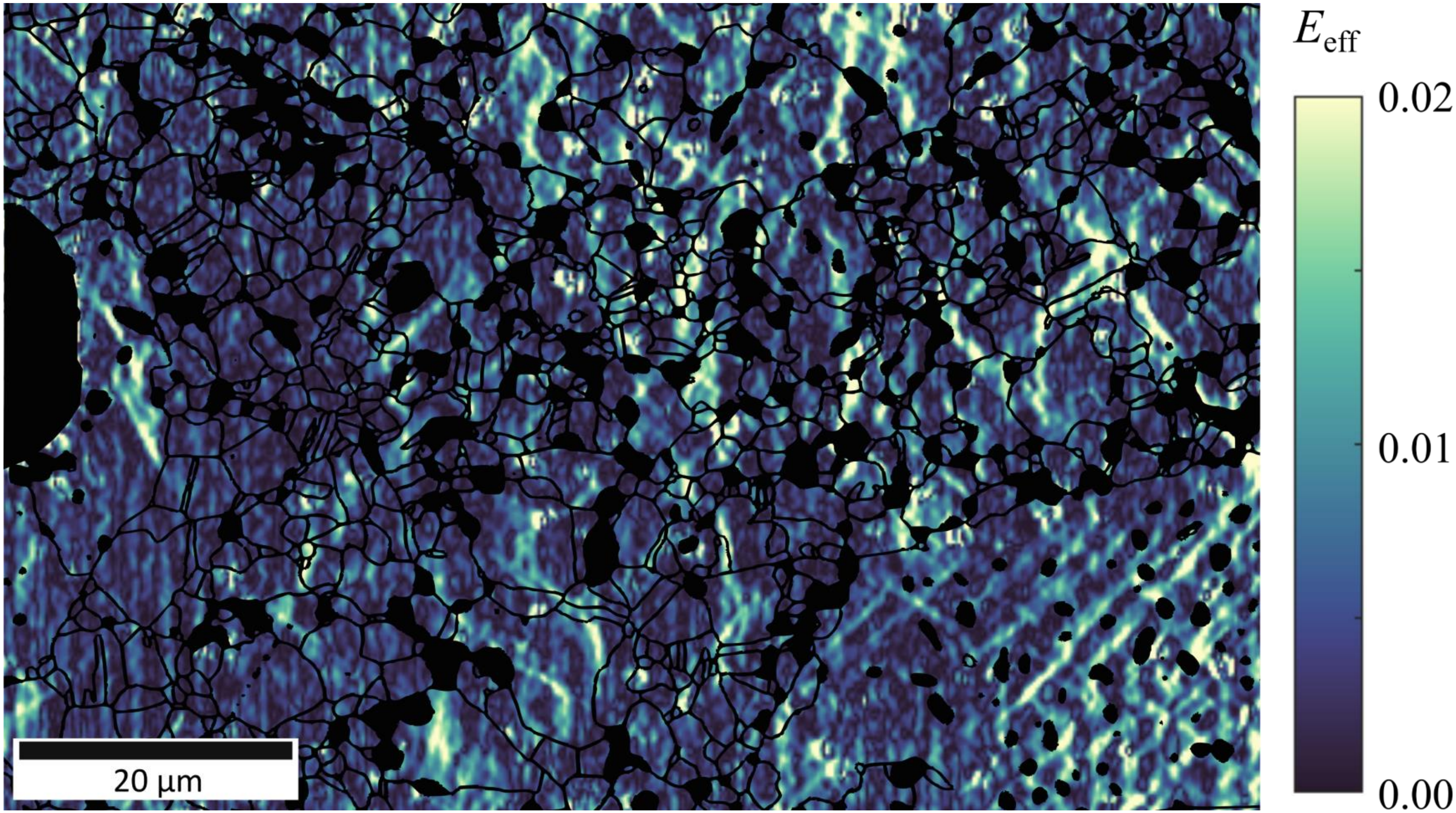

20 µm
E_{eff}
0.02
0.01
0.00

Focus on large grain regions

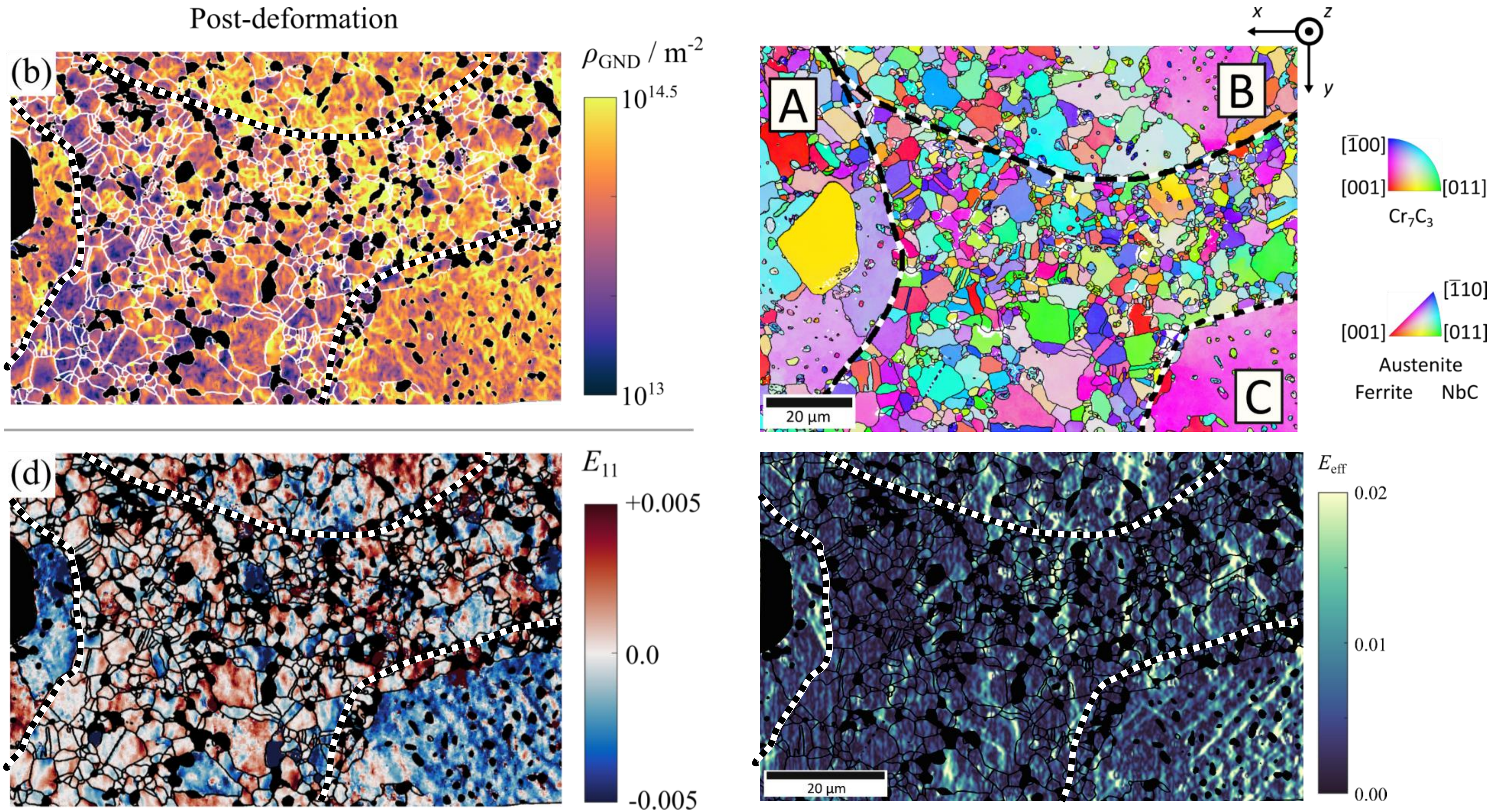

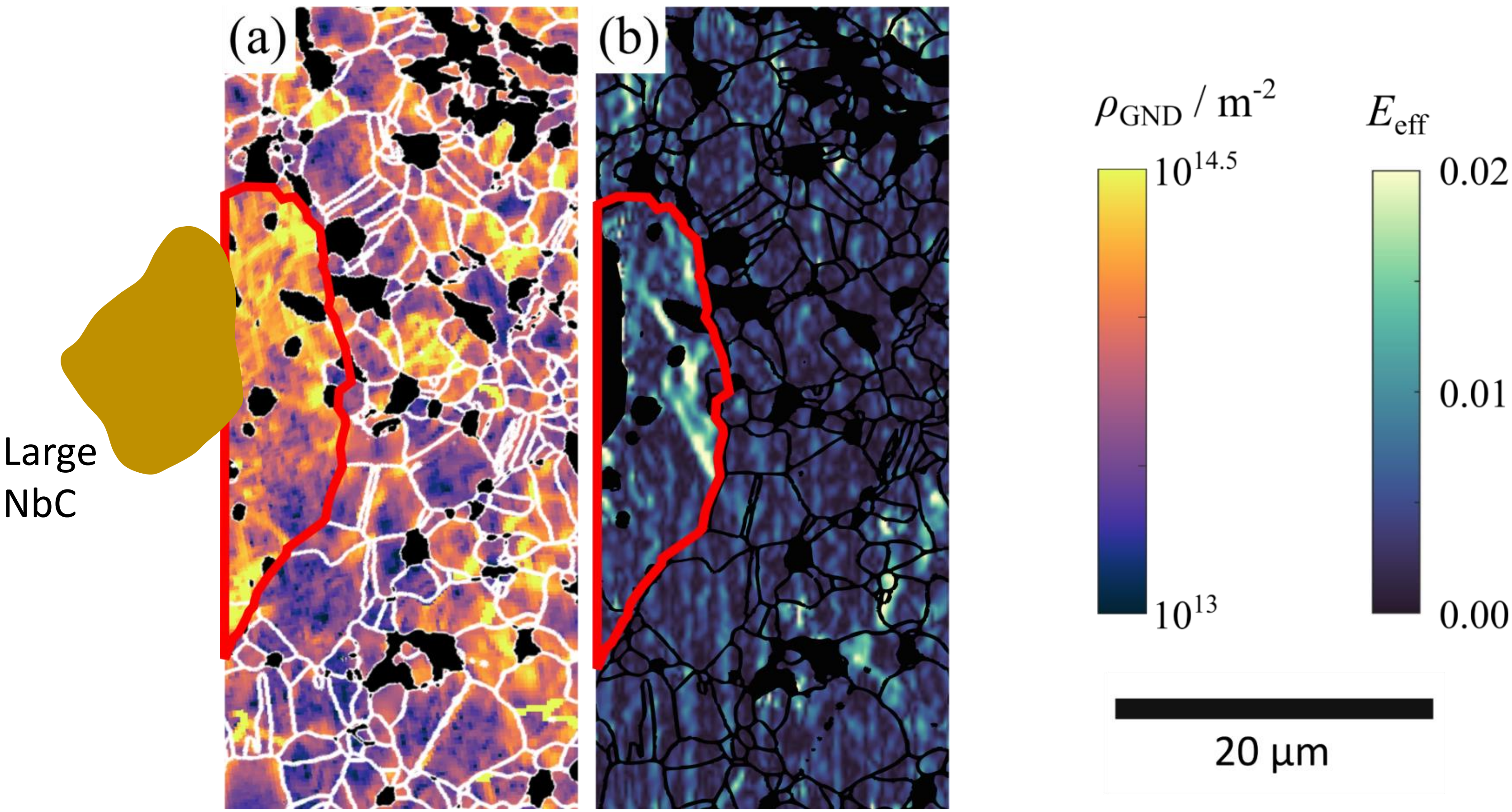

What are the implications on wear and galling performance?

Conclusions – Nitronic 60

- Highly heterogeneous deformation owing to large grains
- Cross-hardening and GND accumulation main hardening mechanisms
- Trends and mechanisms nearly identical at RT and 300°C
    - Slight increase in strain with temperature

❖ Key point: results all show little change from room temperature

Conclusions – Tristelle 5183

- Complex microstructure → complex micromechanics!
- Fine grains with dispersed ferrite/carbides beneficial
- Large austenite grains deleterious

❖Key point: results all show little change from room temperature[+]

[+] RT results not shown here, see Zhao et al. "A comparative assessment of iron and cobalt-based hard-facing alloy deformation using HR-EBSD and HR-DIC." *Acta Materialia* 159 (2018): 173-186.

So what's causing the change?

Change in material properties?	Somewhat
Micromechanical matrix deformation?	Somewhat
Internal heat generation?*	No
Frictional heat generation?*	No
Oxide/contaminant layers?	?
Particle pull-out	?

*Poole, B., Barzdajn, B., Dini, D., Stewart, D., & Dunne, F. P. (2020). The roles of adhesion, internal heat generation and elevated temperatures in normally loaded, sliding rough surfaces. *International Journal of Solids and Structures*, *185*, 14-28.

Acknowledgements

Dr Stewart, Prof. Dini, Prof. Dunne
EPSRC, UKRI & Rolls-Royce plc.
Ben Wood – grip machining & electronics
Alex Bergsmo & Paul Wan– rig & DIC co-conspirators

And…
Imperial, Cambridge, Open CDT in Nuclear Energy
Engineering Alloys Theme
Micromechanics Research Group

?